# ON RIEMANN SOLUTIONS TO WEAKLY HYPERBOLIC SYSTEMS: PART 1. MODELLING SUBCRITICAL FLOWS IN ARTERIES

EE HAN*, GERALD WARNECKE †, ELEUTERIO F. TORO ‡, AND ANNUNZIATO SIVIGLIA §

**Abstract.** The Riemann solutions to a reduced $3 \times 3$ mathematical model governing blood flow in medium to large size vessels with discontinuous material properties are constructed in a uniform manner for the case of subcritical initial data. A tube law involving discontinuous mechanical properties is used to close the system. Consequently, the task of constructing the Riemann solutions becomes very complicated and challenging. Two combined wave curves in the state space named L–M and R–M curves are defined in order to deal with resonance or weak hyperbolicity of the governing system. The classification of the L–M and R–M curves depends on the existence and monotonicity of two basic composite wave curves, which are analyzed in complete detail. All possible wave configurations with classical and resonant waves are studied in detail. Moreover, the cases of vessel collapse are also included, even though for the case of arteries, under physiological conditions, this is only of academic value. The resulting Riemann solution comprehensively explains the effects of rapid and discontinuous change of material properties on the velocity of blood flows and the cross sectional area of blood vessels. In the future, the Riemann-problem solutions obtained here could be of use for constructing useful numerical schemes for solving the initial-boundary value problem for complex vessel networks.

**Key words.** Blood flows, physiological flows, Riemann problem, subcritical speed index, shock, rarefaction, resonant wave, L–M curve, R–M curve

**AMS subject classifications.** 76Z05, 35L03, 35L60

## 1. Introduction.

Models for the physiological flows through flexible tubes are a rich source of interesting mathematical problems associated with partial differential equations. In particular, a simplification of the full fluid-structure interaction problem that describes the interactions between the pressure of the fluid and compliant walls gives rise to non-linear hyperbolic systems. For background see, for example, [16], [27], [28], [9], [8], and references therein. When the material properties that characterize blood vessels, such as the Young's modulus, are constant, then such systems are strictly hyperbolic, have conservative form, their solutions are well understood and satisfactory numerical methods can be devised; see [31], [4], [1], and [22] for instance.

Difficulties arise when one attempts to include geometrical and mechanical properties which vary rapidly or even discontinuously, such as in stenosed or stented vessels. In these cases an abrupt variation of the undistorted cross-sectional area or an abrupt variation of the Young's modulus of the vessel wall can induce transitions through the critical state. Then a complex cross-sectional profile appears where both subcritical and supercritical conditions appear [29], [18].

Recently, Toro and Siviglia [32] put forward a mathematical model that consists

*Institute for Analysis and Numeric, Otto-von-Guericke-University Magdeburg, Germany (eehan84@yahoo.com).

†Institute for Analysis and Numeric, Otto-von-Guericke-University Magdeburg, Germany (gerald.warnecke@ovgu.de).

‡Laboratory of Applied Mathematics, Faculty of Engineering, University of Trento, Italy (toro@ing.unitn.it).

§Laboratory of Hydraulics, Hydrology and Glaciology (VAW), ETH Zurich (siviglia@vaw.baug.ethz.ch).

of a $3 \times 3$ first-order non-conservative system. It is given as

$$\begin{aligned} &\partial_t A + \partial_x(Au) = 0, \\ &\partial_t(uA) + \partial_x(Au^2 + \tfrac{A\Psi}{\rho}) - \tfrac{\Psi}{\rho}\partial_x A = 0, \\ &\partial_t K = 0, \end{aligned} \tag{1.1}$$

where $A(x,t)$ is the cross sectional area of the blood vessel, $u(x,t)$ is the averaged velocity of blood for the cross section, $\rho$ is the blood density assumed to be constant, $\Psi$ and $K$ represent the *transmural pressure* and time-independent material properties of the blood vessel respectively. Usually, several other terms are added to take into account, for example, viscous resistance of the flow per unit length of the blood vessel, body forces, and the other properties of the cardiovascular system, see e.g. [32, 4, 5]. Here we neglect all these effects. For a model that includes more physical parameters see [33]. A constitutive relation, named the tube law, is required to close the system (1.1), and is given as

$$\Psi(A;K) := p - p_e = K(x)\left[\left(\frac{A}{A_0}\right)^m - 1\right]. \tag{1.2}$$

Here $p$ is the pressure due to the force exerted by the vessel walls and the pumping action of the heart, while $p_e$ is the external pressure at which the cross sectional area and the radius of the tube reach an equilibrium state, i.e. $A = A_0$ and $R = R_0$. For the sake of simplicity, in this work $p_e$ and $m$ are assumed to be constant. In particular, the parameter $m = \frac{1}{2}$ correctly describes wave propagation patterns in networks of arteries, as extensively reported in the existing literature [1, 23].

The first-order system (1.1) is resonant hyperbolic; see [32], [15] and [25]. Weak solutions to resonant hyperbolic systems have been defined in the theory introduced by Dal Maso, LeFloch and Murat in [7]. Due to the non–conservative terms, the strict hyperbolicity and uniqueness are lost. This common feature can also be found in the other well–known resonant hyperbolic systems; see, e.g. [25, 15, 26, 14, 19, 2, 3, 20, 30, 21, 11, 10]. Mathematically, resonant hyperbolic systems can be decoupled into a strictly hyperbolic part and a stationary source part. The strictly hyperbolic part has been extensively studied in the literature; see [22, 31] and references therein. The stationary source part, however, entirely depends on the physical process that the model describes. Moreover, the resonance is very difficult to analyze under a uniform framework due to the coincidence of the stationary source and one of the nonlinear wave families of the strictly hyperbolic part.

In this paper we carry out a mathematical study of (1.1). According to [32], the mathematical structure of (1.1) is similar to other well studied resonant hyperbolic systems, e.g. the shallow water equations with bottom topography [20, 10] and the isentropic gas dynamic equations in a nozzle with variable cross-sectional area [26, 14, 19]. The framework for the construction of the Riemann solutions to these entirely different models is similar. However the challenge for incorporating the resonance in the system is different from model to model. This leads to a considerable body of literature on the topic of the Riemann problem of resonant hyperbolic systems.

LeFloch and Thanh investigated the Riemann problem for the shallow water equations with discontinuous bottom topography in [20, 21]. There they studied existence and uniqueness of the Riemann solutions based on the possible mutual positions of the wave curves in the state plane. However they omitted one possible type of solutions, which is denoted as the wave configuration $E$ in [10]. Moreover they did not give complete proofs for the existence and uniqueness of the solutions.

Especially for the conjectures in [21, Remark 4, p. 7641, Remark 6, p. 7646]. It is worth remarking that the numerical solution by the Godunov scheme proposed by them converged to the wrong solution in their test 7; see [21, p. 7658]. They concluded that this phenomenon was due to a limitation of the physical model itself, rather than due to an error in the exact Riemann solver. The analogous construction for the Riemann solution to the equations of gas dynamics in a nozzle with discontinuous cross-sectional area can be found in [19, 30].

Recently, inspired by Marchesin and Paes-Leme in [26], Han et al. [11, 10] completely solved the Riemann problem for the equations of gas dynamics in a nozzle with discontinuous cross-sectional area and the shallow water equations with discontinuous bottom topography respectively. In [11, 10], a velocity function was introduced to get rid of the stationary wave curves. The existence and monotone behavior of the velocity function played a crucial role in the classification of the cases of the Riemann problem. The composite wave curves were defined in the state plane for the construction of solutions to Riemann problems. The multiplicity of Riemann solutions was attributed to the bifurcation on the composite wave curves in the state plane. This makes the approach in [11, 10] to the Riemann solutions different from the previous work in [19, 30, 21]. In addition, the existence and uniqueness of the Riemann solutions for corresponding models have been completely established for any given Riemann initial data under the framework in [11, 10].

The present work is devoted to the complete construction of the Riemann solution for the $3 \times 3$ first–order nonlinear resonant hyperbolic system (1.1) following [11, 10]. Note that the tube law (1.2), which is analogous to the equation of state in gas dynamics, see e.g. [24, 30, 11], involves the mechanical property variable $K$. For the Riemann problem we consider the variable $K$ is discontinuous. This makes the construction of the Riemann solutions very challenging, much more so than for the analogous extended systems for shallow water with discontinuous bottom topography [20, 21, 10] and gas dynamics equations in ducts with continuous equation of state [30, 11]. For the mathematical complications of the Riemann problem for homogeneous gas dynamics systems with non-smooth equation of state, we refer to [6] and references therein.

The Riemann solutions without the resonant waves have been partially studied by Toro and Siviglia in [32]. There they neglected the resonant waves. According to [32], there exist three elementary waves for the governing system. One is the stationary wave which is associated to a linearly degenerate characteristic field due to jump discontinuities of geometrical and mechanical properties of the blood vessels, e.g. external pressures, muscle forces, wall thickness, and Young's modulus etc. The remaining two elementary waves are nonlinear waves which are distinct from each other and associated to genuinely nonlinearly characteristic fields. The nonlinear waves consist of shocks and rarefactions.

The stationary wave curves are deduced from the nonlinear velocity function. In order to completely solve the Riemann problem, the stationary wave curve was attached to two nonlinear wave curves. These combined wave curves are defined as the L–M and R–M curves, since they are the set of intermediate states related to the left and right given Riemann initial data. In addition, the types of the wave configurations are determined by the existence and monotonicity of two basic composite wave curves. Due to them, as well as the complicated tube law (1.2), a number of critical values are introduced; these depend on the equilibrium states, the ratio of mechanical properties and the blood vessel areas. The relations of these critical values, the subcritical and

the supercritical speed index of the Riemann initial data are used to classify the cases of the L–M and R–M curves.

In this work, we only focus on the Riemann solution to the subcritical speed index initial data cases in order to restrict the length of the paper. The Riemann solution for the supercritical speed index cases will be presented in a follow up paper [12]. Concerning the Riemann problem with subcritical initial data, the L–M and R–M curves are continuous as well as monotone decreasing and increasing, respectively. Therefore the Riemann solution uniquely exists. Several examples are used to illustrate this point. Moreover the exact Riemann solutions obtained can be directly applied as reference solutions to assess the performance of numerical schemes. They also reveal the specific wave propagation and interactions of the model coupled with tube laws having discontinuous material properties. A special phenomenon occurs, that both the inflow and the outflow states are critical states for certain cases; this is due to the admissible jump of the variable accounting for mechanical properties. This phenomenon can never occur in the other well–known resonant hyperbolic systems with smooth constitutive relations. The current one-dimensional model is an integral component of large multi-scale models for the cardiovascular system [28]. Therefore this work will help in the development of models to simulate realistic configurations of the human circulation system.

In addition we have to point out that the exact Riemann solution constructed in this work is a weak solution under the theory introduced in [7]. For details we refer to [13]. Moreover, the present results only works for the parameter $m$ in region $]0, 1[$ under an extra conjecture given in [12, Assumption 3.15].

This paper is organized as follows. In Section 2 we introduce the model and analyze its mathematical properties. Here three distinct elementary waves and their properties are studied. In Section 3 we first focus on the behavior of the two basic composite wave curves. Based on them, we classify and formulate the L–M and R–M curves. Several examples for different wave configurations are presented. Conclusions are drawn in Section 4.

**2. Model and mathematical properties.** One dimensional blood flows in medium to large diameter compliant vessels can be regarded as continuum and incompressible flows in thin–walled collapsible tubes. A simplified $3 \times 3$ system (1.1) was proposed by Toro and Siviglia in [32] along with the tube law (1.2), with the mechanical property variable $K(x)$ taken as

$$K(x) = \frac{\sqrt{\pi}}{(1-\nu^2)R_0}\frac{Eh}{\sqrt{A_0}},$$

where the additional variable $h$ is the thickness of the vessel wall, $E$ is the *Young's modulus* of elasticity, and $\nu$ is the Poisson ratio.

Following Ku [17], we define the local elastic tube pressure wave speed of (1.1) as

$$c(A, K) := \sqrt{\frac{A}{\rho}\Psi_A} = \sqrt{\frac{mK}{\rho}\left(\frac{A}{A_0}\right)^m}. \tag{2.1}$$

It is analogously to the sound speed in gas dynamics, see [11]. In addition the ratio of local velocity to local tube wave speed is named *speed index* given as

$$S^I = \frac{u}{c}. \tag{2.2}$$

The superscript $I$ is used to distinguish $S^I$ from the other variables related to the wave speed. This speed index is analogous to Mach number or Froude number in the fluid mechanics. Specifically, we say that the blood flow is subcritical if $|S^I| < 1$; It is supercritical if $|S^I| > 1$; And it is critical if $|S^I| = 1$.

Note that if $K$ is constant, then (1.1) is a $2 \times 2$ conservative strictly hyperbolic system. In this case the Riemann solutions are well established, see e.g. Toro [31], LeVeque [22], Brook et al. [4], etc. Hereafter, we always assume that $K$ is not constant. Then the quasi linear form of the system (1.1) is

$$\mathbf{W}_t + \mathbf{A}(\mathbf{W})\mathbf{W}_x = \mathbf{0},$$

where $\mathbf{W} = (A,\ u,\ K)^T$ and the *Jacobian matrix* $\mathbf{A}(\mathbf{W})$ is in the form

$$\mathbf{A}(\mathbf{W}) = \begin{pmatrix} u & A & 0 \\ \frac{\Psi_A}{\rho} & u & \frac{\Psi_K}{\rho} \\ 0 & 0 & 0 \end{pmatrix}.$$

The three eigenvalues of the Jacobian matrix $\mathbf{A}(\mathbf{W})$ are

$$\lambda_0 = 0, \quad \lambda_1 = u - c, \quad \lambda_2 = u + c.$$

The system (1.1) is weakly hyperbolic as a result of the fact that $\lambda_0$ can coincide with the other two eigenvalues. The corresponding right eigenvectors are

$$\mathbf{R}_0 = \begin{pmatrix} 1 \\ 0 \\ \frac{(u^2-c^2)}{c^2} \end{pmatrix}, \qquad \mathbf{R}_1 = \begin{pmatrix} 1 \\ u-c \\ 0 \end{pmatrix}, \qquad \mathbf{R}_2 = \begin{pmatrix} 1 \\ u+c \\ 0 \end{pmatrix}.$$

Direct calculation yields that

$$\mathbf{R}_0 \to (1,0,0)^T, \quad \mathbf{R}_j \to (1,0,0)^T \quad \text{as } \lambda_j \to 0 \text{ for } j = 1, 2.$$

Consequently the system (1.1) is degenerate at the critical states $u = \pm c$. It is a resonant or weakly hyperbolic system.

The Riemann initial data of (1.1) are two piecewise constant data given as follows

$$(K, A, u)(x, 0) = \begin{cases} (K_L,\ A_L,\ u_L), & x < 0, \\ (K_R,\ A_R,\ u_R), & x > 0, \end{cases} \tag{2.3}$$

Without loss of generality, let $c_L = c(A_L, K_L)$ and $c_R = (A_R, K_R)$ denote, respectively, the local elastic tube pressure wave speed of the left and right Riemann initial data.

Concerning the Riemann solutions to (1.1) and (2.3), there are three different elementary waves associated to the corresponding characteristic fields. We use $j$-waves, $j = 0, 1, 2$, to denote the waves associated to the $j$–characteristic fields when the eigenvalues are distinct from each other. Specifically the 1– and 2–waves are shocks or rarefactions. The 0-wave is a stationary wave due to the jump of the parameter $K$ at $x = 0$. When a shock or a rarefaction does not coincide with the stationary wave, i.e. they are not located at or across the line $x = 0$, the parameter $K$ is constant across these nonlinear waves. Toro and Siviglia in [32] derived the Rankine–Hugoniot conditions and the Riemann invariants for shocks and rarefactions respectively. We shortly recall the shock and rarefaction curves in the next section. The detailed derivation can be found in [32].

**2.1. Shock and rarefaction curves.** Let $\mathbf{w}_q = (A_q, u_q)^T$ be any state in state space and $j = 1, 2$ represent the number of the wave family. Assume that the state $\mathbf{w} = (A, u)^T$ is connected to $\mathbf{w}_q$ by a $j$–shock. Then the shock speed $\sigma_j$ and the velocity $u$ can be expressed as follows

$$\sigma_j(A; \mathbf{w}_q) = u_q \pm \frac{c_q}{\sqrt{m+1}} \left[ \frac{\left(\frac{A}{A_q}\right)^{m+1} - 1}{1 - \frac{A_q}{A}} \right]^{\frac{1}{2}}, \tag{2.4}$$

$$u = u_q \pm \frac{c_q}{\sqrt{m+1}} \left[ \left( \left(\frac{A}{A_q}\right)^{m+1} - 1 \right) \left(1 - \frac{A_q}{A}\right) \right]^{\frac{1}{2}}, \tag{2.5}$$

where $A > A_q$, $\sigma_j$ and $u$ takes $-$ when $j = 1$ and $+$ when $j = 2$ in (2.4) and (2.5). We use admissible shock curves $S_j(\mathbf{w}_q)$ to denote states that can be connected to $\mathbf{w}_q$ by a $j$–shock given by

$$S_j(\mathbf{w}_q) = \left\{ (A, u) \mid u = u_q \pm \tfrac{c_q}{\sqrt{m+1}} \left[ \left( \left(\tfrac{A}{A_q}\right)^{m+1} - 1 \right) \left(1 - \tfrac{A_q}{A}\right) \right]^{\frac{1}{2}} \text{ with } A > A_q \right\}.$$

For any given state $\mathbf{w}_q$ with $A_q > 0$, assume that $\mathbf{w} \in S_j(\mathbf{w}_q)$, then the following Lax entropy conditions can be established for 1– and 2–shocks:

$$u - c < \sigma_1(A; \mathbf{w}_q) < u_q - c_q, \tag{2.6}$$

and

$$u_q + c_q < \sigma_2(A; \mathbf{w}_q) < u + c.$$

With particular emphasis we investigate subset of states $S_j^0(\mathbf{w}_q)$ given as

$$S_j^0(\mathbf{w}_q) = \{ \mathbf{w} \mid \mathbf{w} \in S_j(\mathbf{w}_q) \text{ and } \sigma_j(A; \mathbf{w}_q) = 0 \}. \tag{2.7}$$

Note that $S_j^0(\mathbf{w}_q)$ refers to the states which can be connected to $\mathbf{w}_q$ by a steady shock, i.e. $\sigma_j(A; \mathbf{w}_q) = 0$. Hence from (2.4), we get

$$\left(\frac{A}{A_q}\right)^{m+2} - \left[1 + (m+1)\left(\frac{u_q}{c_q}\right)^2\right]\left(\frac{A}{A_q}\right) + (m+1)\left(\frac{u_q}{c_q}\right)^2 = 0. \tag{2.8}$$

This motivates a function $F(x)$ with respect to $x = \frac{A}{A_q} > 1$ given by

$$F(x) := x^{m+2} - \left[1 + (m+1)\left(\frac{u_q}{c_q}\right)^2\right] x + (m+1)\left(\frac{u_q}{c_q}\right)^2. \tag{2.9}$$

Note that

$$F'(x) = (m+2)x^{m+1} - \left[1 + (m+1)\left(\frac{u_q}{c_q}\right)^2\right].$$

We introduce the value

$$x^* = \left[ \frac{1 + (m+1)\left(\frac{u_q}{c_q}\right)^2}{m+2} \right]^{\frac{1}{m+1}},$$

and obtain the fact that $x^* > 1$ due to $\left(\frac{u_q}{c_q}\right)^2 > 1$. Moreover the function $F(x)$ is decreasing when $x < x^*$ and increasing when $x > x^*$. Furthermore we have

$$\begin{aligned} F(x^*) &= (m+1)\left\{ \left(\frac{u_q}{c_q}\right)^2 - \left[ \frac{1+(m+1)\left(\frac{u_q}{c_q}\right)^2}{m+2} \right]^{\frac{m+2}{m+1}} \right\} \\ &< 0. \end{aligned}$$

Hence the equation $F(x) = 0$ with $x > x^* > 1$ always has a unique solution. We denote it as $x_{s_j^0}$. It can be calculated by iteration methods. Therefore the set of states $S_j^0(\mathbf{w}_q)$ contains only one state denoted as

$$\hat{\mathbf{w}}_{j,q} = S_j^0(\mathbf{w}_q) \quad j = 1, 2. \tag{2.10}$$

The components of $\hat{\mathbf{w}}_{j,q}$ can be calculated by

$$\hat{A}_{j,q} = A_q x_{s_j^0}, \quad \hat{u}_{j,q} = \frac{A_q u_q}{\hat{A}_{j,q}}. \tag{2.11}$$

Similarly, we use $R_j(\mathbf{w}_q)$ to denote the set of states which can be connected to the given state $\mathbf{w}_q$ by a $j$–rarefaction, i.e.

$$R_j(\mathbf{w}_q) = \left\{ \mathbf{w} \mid u = u_q \pm \tfrac{2}{m}(c - c_q) \text{ with } A \le A_q \right\}.$$

The nonlinear 1– and 2–waves consist of shocks and rarefactions. Therefore the corresponding wave curves denoted as $T_1(\mathbf{w}_L)$ and $T_2(\mathbf{w}_R)$, respectively, can be described entirely as a one parameter family of states given as

$$T_1(\mathbf{w}_q) = \{\mathbf{w} | u = u_L - f(A; \mathbf{w}_L),\ A > 0\}, \tag{2.12}$$
$$T_2(\mathbf{w}_q) = \{\mathbf{w} | u = u_R + f(A; \mathbf{w}_R),\ A > 0\}, \tag{2.13}$$

where

$$f(A; \mathbf{w}_q) := \begin{cases} \frac{2}{m}\left( \sqrt{\frac{mK_q}{\rho}\left(\frac{A}{A_0}\right)^m} - c_q \right), & \text{if } A \le A_q, \\ \frac{c_q}{\sqrt{m+1}} \left[ \left( \left(\frac{A}{A_q}\right)^{m+1} - 1 \right)\left(1 - \frac{A_q}{A}\right) \right]^{\frac{1}{2}}, & \text{if } A > A_q. \end{cases} \tag{2.14}$$

More important, the following lemma holds.

LEMMA 2.1. *Assume that $0 < m < 1$, then the 1–wave curve $T_1(\mathbf{w}_L)$ is strictly decreasing and convex, while the 2–wave curve $T_2(\mathbf{w}_R)$ is strictly increasing and concave in the $(u, A)$ state plane.*

*Proof.* Note that the behaviors of $T_1(\mathbf{w}_L)$ in (2.12) and $T_2(\mathbf{w}_R)$ in (2.13) are entirely determined by the nonlinear function $f(A; \mathbf{w}_q)$. So it is enough to prove

that the function $f(A;\mathbf{w}_q)$ is monotone increasing and concave for $0 < m < 1$. The derivative of the function $f(A;\mathbf{w}_q)$ is

$$f'(A;\mathbf{w}_q) := \begin{cases} \dfrac{\sqrt{\frac{mK_q}{\rho}\left(\frac{A}{A_0}\right)^m}}{A}, & \text{if } A \le A_q, \\ \dfrac{c_q}{2A_q\sqrt{m+1}} \dfrac{(m+1)\left(\frac{A}{A_q}\right)^m - m\left(\frac{A}{A_q}\right)^{m-1} - \left(\frac{A_q}{A}\right)^2}{\sqrt{\left(\left(\frac{A}{A_q}\right)^{m+1}-1\right)\left(1-\frac{A_q}{A}\right)}}, & \text{if } A > A_q. \end{cases} \tag{2.15}$$

Note that when $A > A_q$ we have

$$f'(A;\mathbf{w}_q) = \frac{c_q}{2A_q\sqrt{m+1}} \frac{m\left(\frac{A}{A_q}\right)^{m-1}\left(\frac{A}{A_q}-1\right) + \left(\frac{A}{A_q}\right)^m - \left(\frac{A_q}{A}\right)^2}{\sqrt{\left(\left(\frac{A}{A_q}\right)^{m+1}-1\right)\left(1-\frac{A_q}{A}\right)}}. \tag{2.16}$$

So (2.15) and (2.16) imply that $f'(A;\mathbf{w}_q) > 0$ and $\lim\limits_{A\to A_q+} f'(A;\mathbf{w}_q) = \frac{c_q}{A_q}$ by l'Hôpital's rule due to both the numerator and denominator of the fraction go to zero. Concerning the concavity we consider the second derivative of the function $f(A;\mathbf{w}_q)$, which is

$$f''(A;\mathbf{w}_q) := \begin{cases} \left(\frac{m}{2}-1\right) A^{\frac{m}{2}-2}\sqrt{\frac{mK_q}{\rho}\left(\frac{1}{A_0}\right)^m}, & \text{if } A \le A_q, \\ \dfrac{c_q}{4A_q^2\sqrt{m+1}} \dfrac{g(A)}{\left[\left(\left(\frac{A}{A_q}\right)^{m+1}-1\right)\left(1-\frac{A_q}{A}\right)\right]^{\frac{3}{2}}}, & \text{if } A > A_q, \end{cases} \tag{2.17}$$

where

$$g(A) = 2\left[m(m+1)\left(\frac{A}{A_q}\right)^{m-1} - m(m-1)\left(\frac{A}{A_q}\right)^{m-2} + 2\left(\frac{A}{A_q}\right)^{-3}\right]\left[\left(\frac{A}{A_q}\right)^{m+1} - \left(\frac{A}{A_q}\right)^m + \left(\frac{A}{A_q}\right)^{-1} - 1\right] - \left[(m+1)\left(\frac{A}{A_q}\right)^m - m\left(\frac{A}{A_q}\right)^{m-1} - \left(\frac{A}{A_q}\right)^{-2}\right]^2 \tag{2.18}$$

On one hand obviously we have $f''(A;\mathbf{w}_q) < 0$ when $A \le A_q$; on the other hand we need to show that $f''(A;\mathbf{w}_q) < 0$ also holds when $A > A_q$. It is enough to confirm this point by verification that $g(A) < 0$ when $A > A_q$. Set $x = \frac{A}{A_q} > 1$, then we have

$$g(x) = x^{-4}\left\{2\left[m(m+1)x^{m+2} - m(m-1)x^{m+1} + 2\right]\left(x^{m+1}-1\right)(x-1) - \left[\left(mx^{m+1}+1\right)(x-1) + x(x^{m+1}-1)\right]^2\right\}.$$

Using the inequality $(a+b)^2 \ge 4ab$ for any $a, b \in \mathbb{R}$ we obtain

$$g(x) \le -\frac{2}{x^4}\left[m(1-m)x^{m+2} + 2\right](x-1)^2\left(x^{m+1}-1\right) < 0,$$

when $0 < m < 1$ and $x > 1$. This establishes the lemma. □

**2.2. Stationary wave curves.** For two states connected by the stationary wave, we use the subscript $_{in}$ to represent the inflow variables while $_{out}$ to represent the outflow variables. Then according to Toro and Siviglia [32], the inflow state and the outflow state satisfy the relations

$$A_{out}u_{out} = A_{in}u_{in}, \tag{2.19}$$

$$\frac{1}{2}\rho u_{out}^2 + K_{out}\left[\left(\frac{A_{out}}{A_0}\right)^m - 1\right] = \frac{1}{2}\rho u_{in}^2 + K_{in}\left[\left(\frac{A_{in}}{A_0}\right)^m - 1\right]. \tag{2.20}$$

From (2.19), we have $\mathrm{sgn}(u_{out}) = \mathrm{sgn}(u_{in})$. Moreover, if $u_{in} = 0$ and

$$A_{in} \geq A_0\left(1 - \frac{K_{out}}{K_{in}}\right), \tag{2.21}$$

then

$$u_{out} = 0, \quad A_{out} = A_0\left[\frac{K_{in}}{K_{out}}\left(\frac{A_{in}}{A_0} - 1\right) + 1\right].$$

Otherwise if (2.21) fails, the outflow state does not exist. The details will be discussed in Section 3.3.3. In the remaining part of this section we always assume that $u_{in} \neq 0$. For the given inflow states $\mathbf{w}_{in}$ as well as the parameters $K_{in}$ and $K_{out}$, our aim is to calculate the outflow state $\mathbf{w}_{out}$.

For simplicity we can use the notation $\mathbf{w}_{out} = \mathbf{J}(K_{out}; \mathbf{w}_{in}, K_{in})$ to represent the explicit solution $\mathbf{w}_{out}$ implicitly given by (2.19) and (2.20), where

$$\begin{cases} K_{in} = K_L, \\ K_{out} = K_R, \end{cases} \quad \text{when } u_{in} > 0, \qquad \begin{cases} K_{in} = K_R, \\ K_{out} = K_L, \end{cases} \quad \text{when } u_{in} < 0. \tag{2.22}$$

Analogously to the shallow water equations [10, 19] and the gas dynamics equations in a nozzle [11, 20], we also take the discontinuous $K$ as the limiting case of piecewise monotonic mechanical property variables with slope going to infinity. A *velocity* function $\phi(u; \mathbf{w}_{in}, K_{in}, K_{out})$ is deduced from inserting (2.19) into (2.20) given by

$$\phi(u; \mathbf{w}_{in}, K_{in}, K_{out}) := \frac{1}{2}\rho u^2 + K_{out}\left[\left(\frac{A_{in}u_{in}}{A_0 u}\right)^m - 1\right] - \frac{1}{2}\rho u_{in}^2 - K_{in}\left[\left(\frac{A_{in}}{A_0}\right)^m - 1\right]. \tag{2.23}$$

The behavior of the velocity function is summarized in the following lemma.

LEMMA 2.2. *Consider*

$$u^* = sgn(u_{in})\left[\frac{mK_{out}}{\rho}\left(\frac{A_{in}|u_{in}|}{A_0}\right)^m\right]^{\frac{1}{m+2}},$$

*then the properties of the velocity function are the following:*

1. *$\phi(u; \mathbf{w}_{in}, K_{in}, K_{out})$ decreases if $u < u^*$;*
2. *$\phi(u; \mathbf{w}_{in}, K_{in}, K_{out})$ increases if $u > u^*$;*
3. *$\phi(u; \mathbf{w}_{in}, K_{in}, K_{out})$ has the minimum value at $u = u^*$. Moreover we have $|u^*| = c^*$, where $c^* = c(K_{out}, A^*)$ is defined in (2.1) and $A^* = \frac{A_{in}u_{in}}{u^*}$.*

*Proof.* The derivative of this function is

$$\frac{\partial \phi}{\partial u}(u; \mathbf{w}_{in}, K_{in}, K_{out}) = \rho u - \frac{mK_{out}}{u}\left(\frac{A_{in}u_{in}}{A_0 u}\right)^m. \tag{2.24}$$

Consequently, we have

$$\frac{\partial \phi(u; \mathbf{w}_{in}, K_{in}, K_{out})}{\partial u} \begin{cases} < 0, & \text{if } u < u^*, \\ = 0, & \text{if } u = u^*, \\ > 0, & \text{if } u > u^*. \end{cases}$$

It follows that the velocity function $\phi(u; \mathbf{w}_{in}, K_{in}, K_{out})$ is decreasing when $u < u^*$ and increasing when $u > u^*$. It has the minimum value at $u = u^*$. By (2.1) and (2.19) we obtain

$$c = \sqrt{\frac{mK_{out}}{\rho}\left(\frac{A}{A_0}\right)^m} = \sqrt{\frac{mK_{out}}{\rho}\left(\frac{A_{in}u_{in}}{uA_0}\right)^m},$$

So we get the formula

$$\frac{\partial \phi}{\partial u}(u; \mathbf{w}_{in}, K_{in}, K_{out}) = \frac{\rho}{u}(u^2 - c^2). \tag{2.25}$$

Specifically $\frac{\partial \phi(u^*; \mathbf{w}_{in}, K_{in}, K_{out})}{\partial u} = 0$, therefore we have $|u^*| = c^*$. □

COROLLARY 2.3. *Lemma 2.2 shows that the equation $\phi(u; \mathbf{w}_{in}, K_{in}, K_{out}) = 0$ may have two, one or no solutions. Further discussions are as follows:*

1. *If $\phi(u^*; \mathbf{w}_{in}, K_{in}, K_{out}) < 0$, the equation $\phi(u; \mathbf{w}_{in}, K_{in}, K_{out}) = 0$ has two solutions. We denote the one closer to 0 as $u_l$ and the other one as $u_r$, let $c_l$ and $c_r$ be the corresponding local elastic tube pressure wave speeds. According to (2.25), $u_l^2 - c_l^2 < 0$ and $u_r^2 - c_r^2 > 0$. Comparing with the gas dynamics equations in a nozzle and the shallow water equations, see [11, 10], the velocity $u_{out}$ of the outflow state $\mathbf{w}_{out}$ is taken to satisfy the following condition*

$$\operatorname{sgn}(u_q^2 - c_q^2) = \operatorname{sgn}(u_{in}^2 - c_{in}^2), \tag{2.26}$$

   *where $q = l$, or $r$.*
2. *If $\phi(u^*; \mathbf{w}_{in}, K_{in}, K_{out}) = 0$, the equation $\phi(u; \mathbf{w}_{in}, K_{in}, K_{out}) = 0$ has exactly one solution $u = u^*$.*
3. *If $\phi(u^*; \mathbf{w}_{in}, K_{in}, K_{out}) > 0$, the equation $\phi(u; \mathbf{w}_{in}, K_{in}, K_{out}) = 0$ has no solution. This implies that there is no outflow state.*

COROLLARY 2.4. *If $u_{in}^2 = c_{in}^2$, then the condition (2.26) cannot be satisfied any more. There exist two solutions to the corresponding stationary wave. One is subcritical and the other is supercritical. How to choose the solution for the corresponding stationary wave in such a case will be discussed in Sections 3.1.4 and 3.3.2.*

**3. L–M and R–M curves.** In this work without loss of generality we always assume that

$$K_L > K_R. \tag{3.1}$$

The opposite case can be treated as a mirror–image problem by setting the velocity in the inverse direction.

The determination of the mutual positions of the elementary waves is achieved by combining the stationary wave curve with the 1– or 2–wave curves. We name them L–M and R–M curves. These two curves can be regarded as an extension of the 1–wave curve $T_1(\mathbf{w}_L)$ and the 2–wave curve $T_2(\mathbf{w}_R)$, see (2.12) and (2.13), respectively. The detailed definition of the L–M and R–M curves can be found in Sections 3.3 and

3.4. They will serve as a building block for the calculation of the Riemann solutions to (1.1) and (2.3). An analogous construction can be found in [10, 11].

There is precisely one stationary wave in a full wave curve from $\mathbf{w}_L$ to $\mathbf{w}_R$ located either on the L–M curve or the R–M curve. From (2.19), we get that the velocity does not change sign across the stationary wave. This leads to the following facts:

1. If the velocity of the stationary wave is positive, then the stationary wave is attached to the L–M curve;
2. If the velocity of the stationary wave is negative, then the stationary wave is attached to the R–M curve.

Hence the L–M and R–M curves will totally degenerate into the nonlinear wave curves, i.e. the 1–wave curve $T_1(\mathbf{w}_L)$ and the 2–wave curve $T_2(\mathbf{w}_R)$, when $u < 0$ and $u > 0$ respectively.

Furthermore, to involve the collapse of vessels, we define the two critical values for the left and right initial data given as

$$u_{col}^L = u_L + \frac{2}{m}c_L, \qquad u_{col}^R = u_R - \frac{2}{m}c_R. \tag{3.2}$$

The condition $u_{col}^L < 0$ implies that the L–M curve in the $(u, A)$ plane meets the line $A = 0$ before the stationary wave is attached to it. In such kind of case the L–M curve degenerates into

$$P^l(\mathbf{w}_L) = \left\{\mathbf{w} | \mathbf{w} \in T_1(\mathbf{w}_L) \text{ with } u \le u_{col}^L\right\}. \tag{3.3}$$

Analogously if $u_{col}^R > 0$, the R–M curve degenerates into

$$P_1^r(\mathbf{w}_R) = \left\{\mathbf{w} | \mathbf{w} \in T_2(\mathbf{w}_R) \text{ with } u \ge u_{col}^R\right\}. \tag{3.4}$$

For the given noncollapsible Riemann initial data $\mathbf{w}_L$ and $\mathbf{w}_R$, if $u_{col}^L < 0$ and $u_{col}^R > 0$, the solution is trivial and has the wave configuration $A_{col}^1$, see Figure 3.13. In it the stationary wave disappears due to the collapse of the vessel around $x = 0$. The example of the Riemann solution is similar to the one given in [32, Fig. 4 ] but with a jump of the material property $K$. The collapsible vessel states are like vacuum states in gas dynamics and dry bed states in shallow water.

In the following we always assume that $u_{col}^L > 0$ and $u_{col}^R < 0$ unless otherwise stated. In such kind of case the L–M curve always contains the segment

$$P_1^l(\mathbf{w}_L) = \{\mathbf{w} | \mathbf{w} \in T_1(\mathbf{w}_L) \text{ with } u < 0\}; \tag{3.5}$$

And the R–M curve has the segment

$$P_1^r(\mathbf{w}_R) = \{\mathbf{w} | \mathbf{w} \in T_2(\mathbf{w}_R) \text{ with } u > 0\}. \tag{3.6}$$

The remaining parts of the L–M and R–M curves contain the resonant waves which are not yet determined.

There are two basic types of resonant waves. One type is due to the coincidence of the stationary wave with the transcritical rarefactions. And the other type is due to the coincidence of the stationary wave with a zero speed shock. It turns out that these two basic resonant waves as well as the remaining resonant waves are entirely associated to two basic composite wave curves. In the following section we will focus on these two composite wave curves.

**3.1. Two basic composite wave curves.** The first basic composite wave curve is classical. It consists of one nonlinear wave followed by a stationary wave. We use $P^j_{ES}(\mathbf{w}_q)$, $j = 1, 2$, to denote this basic composite wave associated with the 1– and 2–wave family respectively. The second basic composite wave curve is resonant due to the coincidence of the stationary wave with a zero speed shock. This zero speed shock will split the stationary wave into two parts. One part is a supercritical stationary wave. The other part is a subcritical stationary wave. Analogously we use $P^j_{s0s}(\mathbf{w}_q)$ to denote the second basic composite wave curve, where the inflow state $\mathbf{w}_q$ must be critical or supercritical.

**3.1.1. The basic wave curve $P^j_{ES}(\mathbf{w}_q)$.** For the subcritical state $\mathbf{w}_q$, $P^j_{ES}(\mathbf{w}_q)$ is defined as

$$P^j_{ES}(\mathbf{w}_q) = \left\{\mathbf{w} | \mathbf{w} = J(K_{out}; \mathbf{w}_-, K_{in}), \mathbf{w}_- \in T_j(\mathbf{w}_q); S^w_j(A_-; \mathbf{w}_q) \gtrless 0, u_- \lesseqgtr 0\right\}, \tag{3.7}$$

where $K_{in}$ and $K_{out}$ were defined in (2.22), and $S^w_j(A_-; \mathbf{w}_q)$ represents the $j$–wave speed, for $j = 1, 2$, given by

$$S^w_j(A_-; \mathbf{w}_q) = \begin{cases} u_- \pm c_-, & A_- \le A_q, \\ \sigma_j(A_-; \mathbf{w}_q), & A_- > A_q. \end{cases}$$

In addition, $P^1_{ES}(\mathbf{w}_q)$ requires that $S^w_1(A_-; \mathbf{w}_q) < 0$ and $u_- > 0$, while $P^2_{ES}(\mathbf{w}_q)$ requires that $S^w_2(A_-; \mathbf{w}_q) > 0$ and $u_- < 0$.

We start with the behavior of $P^1_{ES}(\mathbf{w}_L)$. Note that $\mathbf{w}_- \in T_1(\mathbf{w}_L)$ and the curve $T_1(\mathbf{w}_L)$ decreases in the $(u, A)$ state plane. To satisfy the restriction $S^w_1(A_-; \mathbf{w}_L) < 0$ and $u_- > 0$, we define two boundary blood vessel cross sectional areas denoted as $A^{P^1_{ES}}_{min}$ and $A^{P^1_{ES}}_{max}$. The minimum blood vessel cross sectional area $A^{P^1_{ES}}_{min}$ corresponds to $S^w_1(A_-; \mathbf{w}_L) = 0$. Since $u_L \le c_L$, we have

$$A^{P^1_{ES}}_{min} = A^c_l. \tag{3.8}$$

Here $A^c_l$ is the blood vessel cross sectional area of the critical state $\mathbf{w}^c_l \in T_1(\mathbf{w}_L)$. Specifically the components of $\mathbf{w}^c_l = (A^c_l, u^c_l)^T$ are

$$A^c_l = A_0 \left(\frac{\rho}{mK_L}\right)^{\frac{1}{m}} \left(\frac{m}{m+2} u_L + \frac{2}{m+2} c_L\right)^{\frac{2}{m}}, \tag{3.9}$$

$$u^c_l = \frac{m}{m+2} u_L + \frac{2}{m+2} c_L. \tag{3.10}$$

The maximum blood vessel cross sectional area denoted as $A^{P^1_{ES}}_{max}$ corresponds to the solution of $u_L - f(A; \mathbf{w}_L) = 0$. From (2.15), the value $A^{P^1_{ES}}_{max}$ can be expressed as

$$A^{P^1_{ES}}_{max} = \begin{cases} A_0 \left(\frac{\rho}{mK_L}\right)^{\frac{1}{m}} \left(\frac{m}{2} u_L + c_L\right)^{\frac{2}{m}}, & \text{if } u_L \le 0, \\ A_{u^0_1}, & \text{if } u_L > 0, \end{cases} \tag{3.11}$$

where $A_{u^0_1}$ is defined later in (3.17) with $j = 1$ and $\mathbf{w}_q = \mathbf{w}_L$.

Analogously, for $P^2_{ES}(\mathbf{w}_q)$ we introduce the minimum blood vessel cross sectional area denoted as $A^{P^2_{ES}}_{min}$ with respect to $S^w_2(A_-; \mathbf{w}_R) = 0$. Specifically it is given as

$$A^{P^2_{ES}}_{min} = A^c_r, \tag{3.12}$$

where

$$A_r^c = A_0 \left(\frac{\rho}{mK_R}\right)^{\frac{1}{m}} \left(-\frac{m}{m+2}u_R + \frac{2}{m+2}c_R\right)^{\frac{2}{m}}, \tag{3.13}$$

$$u_r^c = \frac{m}{m+2}u_R - \frac{2}{m+2}c_R. \tag{3.14}$$

The maximum blood vessel cross sectional area denoted as $A_{max}^{P_{ES}^2}$ corresponds to the solution to $u_R + f_R(A; \mathbf{w}_R) = 0$. We have

$$A_{max}^{P_{ES}^2} = \begin{cases} A_0 \left(\frac{\rho}{mK_R}\right)^{\frac{1}{m}} \left(-\frac{m}{2}u_R + c_R\right)^{\frac{2}{m}}, & \text{if } u_R \geq 0, \\ A_{u_2^0}, & \text{if } u_R < 0, \end{cases} \tag{3.15}$$

where $A_{u_2^0}$ will be defined later in (3.17) with $j = 2$ and $\mathbf{w}_q = \mathbf{w}_R$.

We now calculate $A_{u_1^0}$ and $A_{u_2^0}$. For $\mathbf{w}_q$, from (2.5) it satisfies

$$0 = u_q \pm \frac{c_q}{\sqrt{m+1}} \left[\left(\left(\frac{A}{A_q}\right)^{m+1} - 1\right)\left(1 - \frac{A_q}{A}\right)\right]^{\frac{1}{2}}.$$

This equals to

$$\left(\frac{A}{A_q}\right)^{m+2} - \left(\frac{A}{A_q}\right)^{m+1} - \left[1 + (m+1)\left(\frac{u_q}{c_q}\right)^2\right]\left(\frac{A}{A_q}\right) + 1 = 0. \tag{3.16}$$

Let $x = \frac{A}{A_q}$ in (3.16), we abstract a nonlinear function

$$H(x) := x^{m+2} - x^{m+1} - \left[1 + (m+1)\left(\frac{u_q}{c_q}\right)^2\right]x + 1.$$

Our aim is to find the solution to $H(x) = 0$ with the restriction that $x > 1$. Direct calculation yields

$$H'(x) = (m+2)x^{m+1} - (m+1)x^m - \left(1 + (m+1)\left(\frac{u_q}{c_q}\right)^2\right),$$

and

$$H''(x) = (m+1)x^{m-1}\left[(m+2)x - m\right].$$

Note that $H''(x) > 0$ when $x > 1$ and $H'(1) = -(m+1)\left(\frac{u_q}{c_q}\right)^2 < 0$. So $H'(x)$ strictly increases from a negative value to $+\infty$ when $x > 1$. There exists a unique solution to $H'(x) = 0$ when $x > 1$. We use $x_0$ to denote it. Moreover $H(1) = -(m+1)\left(\frac{u_q}{c_q}\right)^2 < 0$. Therefore the function $H(x)$ first decreases from a negative value $H(1)$ to $H(x_0)$ when $x$ varies from 1 to $x_0$, then it increases from $H(x_0)$ to $+\infty$ when $x$ varies from $x_0$ to $+\infty$. So when $x > 1$ the equation $H(x) = 0$ has a unique solution in the region $x > x_0$. We denote it as $x_{u_j^0}$, which can be calculated by an iteration method. Then the corresponding blood vessel cross sectional area is

$$A_{u_j^0} = A_q x_{u_j^0}. \tag{3.17}$$

According to Remark 2.3 the stationary state $\mathbf{w} = J(K_{out}; \mathbf{w}_-, K_{in})$ may not exist. We study the existence and monotonicity of $P_{ES}^j(\mathbf{w}_q)$ in the subsequent section.

**3.1.2. Existence of $P^j_{ES}(\mathbf{w}_q)$ with $u_q^2 < c_q^2$.** With the aid of Lemma 2.2, the existence of $\mathbf{w} = J(K_{out}; \mathbf{w}_-, K_{in})$ is equivalent to the minimum value of the corresponding velocity function being not positive. Specifically it is given by

$$\frac{m+2}{2m}\rho\left(\frac{K_{out}}{K_{in}}u_-^m c_-^2\right)^{\frac{2}{m+2}} - \frac{1}{2}\rho u_-^2 - \frac{\rho}{m}c_-^2 + K_{in} - K_{out} \leq 0. \tag{3.18}$$

We introduce the function

$$U(A; \mathbf{w}_q) := u_q \pm f(A; \mathbf{w}_q),$$

where $f(A; \mathbf{w}_q)$ is defined in (2.15). Due to $\mathbf{w}_- \in T_j(\mathbf{w}_q)$, the inequality (3.18) suggests to introduce a function given by

$$\begin{aligned}\Omega_q(A; \mathbf{w}_q, K_{in}, K_{out}) \quad := \quad & \tfrac{m+2}{2}\left(\tfrac{\rho}{m}\right)^{\frac{m}{m+2}} K_{out}^{\frac{2}{m+2}}\left(\tfrac{AU(A;\mathbf{w}_q)}{A_0}\right)^{\frac{2m}{m+2}} - \tfrac{\rho U(A;\mathbf{w}_q)^2}{2} \\ & -K_{in}\left(\tfrac{A}{A_0}\right)^m + K_{in} - K_{out},\end{aligned} \tag{3.19}$$

where $q = l, r$, and $K_{in}$ and $K_{out}$ were defined in (2.22), i.e. we have two functions $\Omega_l(A; \mathbf{w}_L, K_L, K_R)$ and $\Omega_r(A; \mathbf{w}_R, K_R, K_L)$.

LEMMA 3.1. *The function $\Omega_q(A; \mathbf{w}_q, K_{in}, K_{out})$ is decreasing if $A^{P^j_{ES}}_{min} < A < A^{P^j_{ES}}_{max}$ and $u_q^2 < c_q^2$.*

*Proof.* It is enough to prove that $\Omega_l(A; \mathbf{w}_L, K_L, K_R)$ is decreasing. The case for $\Omega_r(A; \mathbf{w}_R, K_R, K_L)$ can be dealt with in the same manner. By virtue of the chain role, the derivative of $\Omega_l(A; \mathbf{w}_L, K_L, K_R)$ is

$$\begin{aligned}\Omega_l'(A; \mathbf{w}_L, K_L, K_R) = & \frac{\rho}{A}\left(\frac{K_R}{K_L}\right)^{\frac{2}{m+2}} c(A)^{\frac{4}{m+2}} U(A; \mathbf{w}_L)^{\frac{m-2}{m+2}} \left[U(A; \mathbf{w}_L) - Af'(A; \mathbf{w}_L)\right] \\ & + \frac{\rho}{A}\left[AU(A; \mathbf{w}_L)f'(A; \mathbf{w}_L) - c(A)^2\right],\end{aligned} \tag{3.20}$$

where $c(A) := c(A, K_L)$ for the sake of clarity. Due to (3.8) we have $A^{P^1_{ES}}_{min} = A_l^c$. On one hand if $A < A_L$ the fact holds that $f'(A; \mathbf{w}_L) = \frac{c(A)}{A}$. Hence we have

$$\Omega_l'(A; \mathbf{w}_L, K_L, K_R) = \frac{\rho c(A)}{A}\left[\left(\frac{K_R}{K_L}\right)^{\frac{2}{m+2}}\left(\frac{U(A; \mathbf{w}_L)}{c(A)}\right)^{\frac{m-2}{m+2}} + 1\right]\left[U(A; \mathbf{w}_L) - c(A)\right]. \tag{3.21}$$

From $U(A; \mathbf{w}_L) - c(A) < U(A_l^c; \mathbf{w}_L) - c(A_l^c) = 0$ when $A > A_l^c$, it directly follows that $\Omega_l'(A; \mathbf{w}_L, K_L, K_R) < 0$ when $A_l^c < A < A_L$. On the other hand, if $A > A_L$ $\Omega_l'(A; \mathbf{w}_L, K_L, K_R)$ is complicated owing to the function $f'(A; \mathbf{w}_L)$ defined in (2.15). From (3.20) it is enough to prove the following two facts when $A_L < A < A^{P^1_{ES}}_{max}$

$$w(A) := U(A; \mathbf{w}_L) - Af'(A; \mathbf{w}_L) < 0, \tag{3.22}$$

and

$$\mu(A) := AU(A; \mathbf{w}_L)f'(A; \mathbf{w}_L) - c(A)^2 < 0. \tag{3.23}$$

First we investigate $w(A)$. Note that

$$\begin{aligned} w'(A) &= -2f'(A;\mathbf{w}_L) - Af^{''}(A;\mathbf{w}_L), \\ &= -\frac{c_L}{4A_L\sqrt{(m+1)\left[\left(\frac{A}{A_L}\right)^{m+1}-\left(\frac{A}{A_L}\right)^{m}+\frac{A_q}{A}-1\right]}}\left\{4\left[(m+1)\left(\frac{A}{A_L}\right)^{m} - m\left(\frac{A}{A_L}\right)^{m-1}\right.\right. \\ &\quad \left.\left. -\left(\frac{A}{A_L}\right)^{-2}\right]\left[\left(\frac{A}{A_L}\right)^{m+1}-\left(\frac{A}{A_L}\right)^{m}+\frac{A_L}{A}-1\right]+\frac{A}{A_L}g(A)\right\}, \end{aligned}$$

where $g(A)$ is given in (2.18). After the simplification we get

$$\begin{aligned} w'(A) &= \beta\left[(m+1)(m+3)\left(\frac{A}{A_L}\right)^{2m+1} - 2(m+1)(m+2)\left(\frac{A}{A_L}\right)^{2m} + m(m+2)\right. \\ &\quad \left(\frac{A}{A_L}\right)^{2m-1} - 2(m+1)(m+2)\left(\frac{A}{A_L}\right)^{m} + 2(2m^2+5m+3)\left(\frac{A}{A_L}\right)^{m-1} \\ &\quad \left. -2m(m+2)\left(\frac{A}{A_L}\right)^{m-2} - \left(\frac{A}{A_L}\right)^{-3}\right] < 0, \end{aligned}$$

where $\beta = -\frac{c_L}{4A_L\sqrt{m+1}}\left\{\left(\frac{A}{A_L}\right)^{m+1} - \left(\frac{A}{A_L}\right)^{m} + \frac{A_L}{A} - 1\right\}^{-\frac{1}{2}}$. So when $A > A_L$ and $u_L < c_L$, with $f'(A_L;\mathbf{w}_L) = \frac{c_L}{A_L}$, we obtain

$$w(A) < w(A_L) \quad = \quad u_L - A_L f'(A_L;\mathbf{w}_L) < 0. \tag{3.24}$$

The inequality (3.24) implies that $U(A;\mathbf{w}_L) - Af'(A;\mathbf{w}_L) < 0$. Due to $f'(A;\mathbf{w}_L) > 0$ and $f^{''}(A;\mathbf{w}_L) < 0$, we have

$$\mu'(A) \quad = \quad \left[U(A;\mathbf{w}_L) - Af'(A;\mathbf{w}_L)\right] f'(A;\mathbf{w}_L) + AU(A;\mathbf{w}_L)f^{''}(A;\mathbf{w}_L) - \frac{mc(A)^2}{A} < 0.$$

It follows that

$$\mu(A) < \mu(A_L) = c_L(u_L - c_L) < 0.$$

Thus we obtain that $\Omega_l'(A;\mathbf{w}_L,K_L,K_R) < 0$ if $u_L < c_L$. This completes the proof of the lemma. □

For the existence of $P_{ES}^1(\mathbf{w}_L)$, we have the following lemma.

LEMMA 3.2. *Assume that $K_L > K_R$, the segment $P_{ES}^1(\mathbf{w}_L)$ in (3.7) cannot exist if*

$$A_{max}^{P_{ES}^1} < A_0\left[1 - \frac{K_R}{K_L}\right]^{\frac{1}{m}}. \tag{3.25}$$

*Proof.* By Lemma 3.1, the existence of the segment $P_{ES}^1(\mathbf{w}_q)$ with $A_{min}^{P_{ES}^1} < A < A_{max}^{P_{ES}^1}$ is equivalent to $\Omega_l(A;\mathbf{w}_q,K_L,K_R) \le 0$. The minimum value of $\Omega_l(A;\mathbf{w}_L,K_L,K_R)$ is

$$\Omega_l(A_{max}^{P_{ES}^1};\mathbf{w}_L,K_L,K_R) = K_L\left[1 - \left(\frac{A_{max}^{P_{ES}^1}}{A_0}\right)^{m}\right] - K_R.$$

Note that if (3.25) is satisfied, we have $\Omega_l(A_{max}^{P_{ES}^1};\mathbf{w}_L,K_L,K_R) > 0$. Therefore by Lemma 3.1, $\Omega_l(A;\mathbf{w}_L,K_L,K_R) > 0$ always holds when $A_{min}^{P_{ES}^1} < A < A_{max}^{P_{ES}^1}$. □

COROLLARY 3.3. *For $K_L > K_R$, the Riemann solution includes the state of tube collapse if $A^{P^1_{ES}}_{max} < A_0 \left[1 - \frac{K_R}{K_L}\right]^{\frac{1}{m}}$.*

LEMMA 3.4. *Assume that $u_L \le c_L$ and that the following condition is satisfied*

$$A^{P^1_{ES}}_{max} \ge A_0 \left[1 - \frac{K_R}{K_L}\right]^{\frac{1}{m}}. \tag{3.26}$$

*We have:*

1. *If $u^c_l > u^{sc}_l$, the segment $P^1_{ES}(\mathbf{w}_L)$ defined in (3.7) always exists, where $u^{sc}_l$ defined in (3.28).*
2. *Otherwise, the existence region for the the segment $P^1_{ES}(\mathbf{w}_L)$ defined in (3.7) is $\tilde{A}_c < A_- < A^{P^1_{ES}}_{max}$, where $\tilde{A}_c$ is the solution to $\Omega_l(A; \mathbf{w}_L, K_L, K_R) = 0$.*

*Proof.* The maximum value of $\Omega_l(A; \mathbf{w}_L, K_L, K_R)$ takes at $A = A^{P^1_{ES}}_{min}$. If $u_L \le c_L$, from (3.8), we get $A^{P^1_{ES}}_{min} = A^c_l$, which is defined in (3.9). Using $U(A^c_l; \mathbf{w}_L) = c(A^c_l, K_L)$ in (3.19) we obtain that

$$\Omega_l(A^c_l; \mathbf{w}_L, K_L, K_R) = \frac{\rho(m+2)}{2m}\left[\left(\frac{K_R}{K_L}\right)^{\frac{2}{m+2}} - 1\right](u^c_l)^2 + K_L - K_R. \tag{3.27}$$

We define

$$u^{sc}_l := \sqrt{\frac{\frac{2m}{\rho(m+2)}(K_R - K_L)}{\left(\frac{K_R}{K_L}\right)^{\frac{2}{m+2}} - 1}}. \tag{3.28}$$

Due to $u^c_l > 0$ and $K_L > K_R$, the inequality $\Omega_l(A^c_l; \mathbf{w}_L, K_L, K_R) \le 0$ suggests that $u^c_l \ge u^{sc}_l$. This is enough for the first statement of the lemma. If $u^c_l < u^{sc}_l$, we have $\Omega_l(A^{P^1_{ES}}_{min}; \mathbf{w}_L, K_L, K_R) > 0$ and $\Omega_l(A^{P^1_{ES}}_{max}; \mathbf{w}_L, K_L, K_R) < 0$. From Lemma 3.1, there exists a unique solution to $\Omega_l(A; \mathbf{w}_L, K_L, K_R) = 0$ for $A \in [A^{P^1_{ES}}_{min}, A^{P^1_{ES}}_{max}]$. This completes the proof of the lemma. □

COROLLARY 3.5. *When $u^c_l = u^{sc}_l$, we have $\Omega_l(A^c_l; \mathbf{w}_L, K_L, K_R) = 0$. From Remark 2.3, the outflow state of the corresponding stationary wave $\mathbf{J}(K_R; \mathbf{w}^l_c, K_L)$ is a critical state. That is to say both the inflow and the outflow states are critical states. To distinguish the critical outflow state from the critical inflow state $\mathbf{w}^c_l$, we use $\mathbf{w}^c_* = \mathbf{J}(K_R; \mathbf{w}^c_l, K_L)$ to denote it. The components of $\mathbf{w}^c_l$ are defined in (3.9) and (3.10). The difference of $\mathbf{w}^c_*$ and $\mathbf{w}^c_l$ comes from the difference of $K_L$ and $K_R$.*

In the same manner, we can obtain the condition for the existence of $P^2_{ES}(\mathbf{w}_R)$ with the subcritical states $\mathbf{w}_R$, i.e. $u_R + c_R \ge 0$. The results are summarized in the following corollary.

COROLLARY 3.6. *Note that $U(A^{P^2_{ES}}_{max}; \mathbf{w}_R) = 0$. So if $K_L > K_R$ we have*

$$\Omega_r(A^{P^2_{ES}}_{max}; \mathbf{w}_R, K_R, K_L) = -K_R\left(\frac{A^{P^2_{ES}}_{max}}{A_0}\right)^m + K_R - K_L < 0.$$

*This implies that the tube cannot collapse in a Riemann solution with negative intermediate velocity under the restriction $K_L > K_R$.*

LEMMA 3.7. *Assume that $u_R + c_R \geq 0$, we define*

$$u_r^{sc} = -\sqrt{\frac{\frac{2m}{\rho(m+2)}(K_L - K_R)}{\left(\frac{K_L}{K_R}\right)^{\frac{2}{m+2}} - 1}},$$

*then the following facts hold:*

1. *If $u_r^c \geq u_r^{sc}$, the segment $P_{ES}^2(\mathbf{w}_R)$ always exists.*
2. *Otherwise the segment $P_{ES}^2(\mathbf{w}_R)$ exists if $\tilde{A}_r^c < A_- < A_{max}^{P_{ES}^2}$, where $\tilde{A}_r^c$ is the solution to $\Omega_r(A; \mathbf{w}_R, K_R, K_L) = 0$.*

**3.1.3. Monotonicity of the segment of $P_{ES}^j(\mathbf{w}_q)$.** We summarize the result in the following lemma.

LEMMA 3.8. *The curve $P_{ES}^1(\mathbf{w}_L)$ is continuously decreasing in $(u, \Psi)$ state plane; while the curve $P_{ES}^2(\mathbf{w}_R)$ is continuously increasing in $(u, \Psi)$ state plane.*

*Proof.* By (1.2) we know that $\Psi = K_R\left[\left(\frac{A}{A_0}\right)^m - 1\right]$ and $\Psi = K_L\left[\left(\frac{A}{A_0}\right)^m - 1\right]$ for the component of $P_{ES}^1(\mathbf{w}_L)$ and $P_{ES}^2(\mathbf{w}_R)$ respectively. So it is enough to prove that $u\frac{du}{dA} < 0$. Note that $A$ and $u$ in (3.7) entirely depend on the variable $A_-$. We turn to prove $u\frac{du}{dA_-} < 0$ and $\frac{d\Psi}{dA_-} > 0$. From (2.23) we have

$$\phi(u; \mathbf{w}_-, K_{in}, K_{out}) = 0,$$

where $K_{in}$ and $K_{out}$ were defined in (2.22). The implicit function theorem implies that

$$u\frac{du}{dA_-} = -\frac{u\frac{\partial\phi}{\partial A_-}}{\frac{\partial\phi}{\partial u}}. \tag{3.29}$$

From (2.25) we have $\frac{\partial\phi}{\partial u} = \frac{\rho}{u}(u^2 - c^2)$, i.e. (3.29) becomes

$$u\frac{du}{dA_-} = -\frac{u^2\frac{\partial\phi}{\partial A_-}}{\rho(u^2 - c^2)}. \tag{3.30}$$

Moreover we obtain

$$\frac{\partial\phi}{\partial A_-} = mK_{out}(A_0u)^m(A_-u_-)^{m-1}w(A_-) + \frac{\rho}{A_-}\mu(A_-).$$

From (3.22) and (3.23) we have $w(A_-) < 0$ and $\mu(A_-) < 0$. It directly follows that $\frac{\partial\phi}{\partial A_-} < 0$. Therefore we obtain that $u\frac{du}{dA_-} < 0$ due to (3.30) and $u^2 < c^2$. Analogously we can prove that $\frac{dA}{dA_-} > 0$. It follows that $u\frac{du}{dA} < 0$. This is sufficient for the proof of the lemma. □

**3.1.4. The basic composite wave curve $P_{s0s}^j(\mathbf{w}_q)$.** It turns out that the basic composite wave curve $P_{s0s}^j(\mathbf{w}_q)$ can be only related to the critical inflow state for the subcritical Riemann initial data, i.e. $u_q^2 = c_q^2$. We use $\mathbf{w}_q^c$ to denote the critical states for the sake of clarity. The corresponding composite wave curve is given by

$$P_{s0s}^j(\mathbf{w}_q^c) = \{\mathbf{w} | \mathbf{w} = \mathbf{J}(K_{out}; \mathbf{w}_+, K);\ \mathbf{w}_+ = S_j^0(\mathbf{w}_-);\ \mathbf{w}_- = \mathbf{J}(K; \mathbf{w}_q^c, K_{in})\ \}, \tag{3.31}$$

where $K \in ]K_{in}, K_{out}[$, $K_{in}$ and $K_{out}$ were defined in (2.22) and $q = l, r$. We address that the stationary wave $\mathbf{w}_- = \mathbf{J}(K; \mathbf{w}_q^c, K_{in})$ is an exception of Corollary 2.3. Note that the condition (2.26) is violated because of the fact that $\text{sgn}\left((u_q^c)^2 - (c_q^c)^2\right) = 0$. Following [11, 10], the stationary wave $\mathbf{w}_- = \mathbf{J}(K; \mathbf{w}_q^c, K_{in})$ takes the supercritical outflow state. The existence of $P_{s0s}^j(\mathbf{w}_q^c)$ are summarized in the following lemma.

LEMMA 3.9. *We have two different cases in terms of $j = 1$ and 2.*

1. *Assume that $u_L < c_L$ and $u_l^c \le u_l^{sc}$ , the curve $P_{s0s}^1(\mathbf{w}_l^c)$ exists if $K$ in (3.31) can vary from $K_l$ to $K_r$, which are defined by*

$$]K_l, K_r[= \begin{cases} ]K_R,\ K_L[, & \text{if } A_l^c \ge A_0, \\ ]K_R,\ \kappa_l^\tau K_L[, & \text{if } A_l^c < A_0 \text{ and } A_0 \le A_{s0s}^{l,c}, \\ \{K_L\}, & \text{if } A_l^c < A_0 \text{ and } A_0 > A_{s0s}^{l,c}. \end{cases} \tag{3.32}$$

*Here*

$$A_{s0s}^{l,c} = A_l^c \left[\frac{m+2}{2}\right]^{\frac{1}{m}}$$

*and $\kappa_l^\tau < 1$ is the solution to $\tau(\kappa; \mathbf{w}_l^c) = 0$, which is defined in*

$$\tau(\kappa; \mathbf{w}_l^c) = \frac{m+2}{2}\kappa^{\frac{2}{m+2}} - \left(\frac{A_0}{A_l^c}\right)^m \kappa - \frac{m+2}{2} + \left(\frac{A_0}{A_l^c}\right)^m. \tag{3.33}$$

2. *Assume that $u_R + c_R \ge 0$ and $u_r^c \le u_r^{sc}$, then the curve $P_{s0s}^2(\mathbf{w}_r^c)$ exists if $K$ in (3.31) can vary from $K_l$ to $K_r$, which are defined as*

$$]K_l,\ K_r[= \begin{cases} ]\kappa_r^\tau K_R,\ K_L[, & \text{if } A_r^c > A_0 \text{ and } \frac{K_L}{K_R} > \kappa_r^\tau, \\ \{K_R\}, & \text{if } A_r^c > A_0 \text{ and } \frac{K_L}{K_R} > \kappa_r^\tau, \\ ]K_R,\ K_L[, & \text{Otherwise,} \end{cases} \tag{3.34}$$

*where $\kappa_r^\tau > 1$ is the solution to $\tau(\kappa; \mathbf{w}_r^c) = 0$.*

*Proof.* It is enough to prove the first statement. We need to identify the existence of $\mathbf{w}_- = J(K; \mathbf{w}_l^c, K_L)$ and $\mathbf{w} = J(K_R; \mathbf{w}_+, K)$. Concerning the existence of $\mathbf{w}_- = J(K; \mathbf{w}_l^c, K_L)$, it is equivalent to

$$\frac{m+2}{2m}\rho\left(\frac{K}{K_L}(u_l^c)^m (c_l^c)^2\right)^{\frac{2}{m+2}} - \frac{1}{2}\rho(u_l^c)^2 - \frac{\rho}{m}(c_l^c)^2 + K_L - K \le 0.$$

Dividing $\frac{\rho(c_l^c)^2}{m}$ and setting $\kappa = \frac{K}{K_L}$, a function with respect to $\kappa$ is introduced given by (3.33).

After short computation, we obtain that $\tau(\kappa; \mathbf{w}_l^c)$ is increasing when $\kappa < \left(\frac{A_l^c}{A_0}\right)^{m+2}$ and decreasing when $\kappa > \left(\frac{A_l^c}{A_0}\right)^{m+2}$. It reaches the maximum value at $\kappa = \left(\frac{A_l^c}{A_0}\right)^{m+2}$ expressed as

$$\tau_{max}^* = \frac{m}{2}\left(\frac{A_l^c}{A_0}\right)^2 + \left(\frac{A_l^c}{A_0}\right)^{-m} - \frac{m+2}{2} \ge 0.$$

Therefore $\tau_{max}^* = 0$ if and only if $A_l^c = A_0$, i.e. we have $\tau(\kappa; \mathbf{w}_l^c) \le 0$ for any $\kappa$. Specifically, for any $K$ satisfies $K_R < K < K_L$, we have $\frac{K_R}{K_L} < \frac{K}{K_L} = \kappa < 1$. Hence the region $\frac{K_R}{K_L} < \kappa < 1$ is the one which we are interesting to.

On one hand if $A_l^c > A_0$, there are two solutions $\kappa_l^\tau$ and $\kappa_r^\tau$ to $\tau(\kappa; \mathbf{w}_l^c) = 0$. Note that $\tau(1; \mathbf{w}_l^c) = 0$. So they satisfy $1 = \kappa_l^\tau < \left(\frac{A_l^c}{A_0}\right)^{m+2} < \kappa_r^\tau$. Due to the behavior of the function $\tau(\kappa; \mathbf{w}_l^c)$, we obtain that $\tau(\kappa; \mathbf{w}_l^c) < 0$ when $\frac{K_R}{K_L} < \kappa < 1$.

On the other hand if $A_l^c < A_0$, we have $\left(\frac{A_l^c}{A_0}\right)^{m+2} < 1$. Note that

$$\tau(0; \mathbf{w}_l^c) = -\frac{m+2}{2} + \left(\frac{A_0}{A_l^c}\right)^m.$$

If $A_0 \le A_{s0s}^{l,c}$, we get $\tau(0; \mathbf{w}_l^c) \le 0$. In such kind of case there are also two solutions $\kappa_l^\tau$ and $\kappa_r^\tau$ to $\tau(\kappa; \mathbf{w}_l^c) = 0$. They satisfy $\kappa_l^\tau < \left(\frac{A_l^c}{A_0}\right)^{m+2} < \kappa_r^\tau = 1$. So $\tau(\kappa; \mathbf{w}_l^c) < 0$ if and only if $\kappa < \kappa_l^\tau$. Otherwise if $A_0 > A_{s0s}^{l,c}$, we have $\tau(0; \mathbf{w}_l^c) > 0$. There are only one solution to $\tau(\kappa; \mathbf{w}_l^c) = 0$ at $\kappa = 1$. Hence if $\kappa < 1$, we always have $\tau(\kappa; \mathbf{w}_l^c) > 0$. In short, under the condition $A_l^c < A_0$ and $A_0 > A_{s0s}^{l,c}$, the state $\mathbf{w}_- = J(K; \mathbf{w}_l^c, K_L)$ exists if and only if $K = K_L$.

Now we turn to the existence of $\mathbf{w} = \mathbf{J}(K_R; \mathbf{w}_+, K)$. This is equivalent to

$$\frac{m+2}{2m}\rho\left(\frac{K_R}{K}u_+^m c_+^2\right)^{\frac{2}{m+2}} - \frac{1}{2}\rho u_+^2 - \frac{\rho}{m}c_+^2 + K - K_R \le 0. \tag{3.35}$$

Analogously, a function $\chi(\kappa; \mathbf{w}_q)$ is deduced from (3.35) given by

$$\chi(\kappa; \mathbf{w}_l^c) := \frac{m+2}{2}\left(\frac{K_R}{\kappa K_L}\right)^{\frac{2}{m+2}}\left(\frac{u_+}{c_+}\right)^{\frac{2m}{m+2}} + \left(1 - \frac{K_R}{\kappa K_L}\right)\left(\frac{A_+}{A_0}\right)^{-m} - \frac{m}{2}\left(\frac{u_+}{c_+}\right)^2 - 1, \tag{3.36}$$

where $\kappa = \frac{K}{K_L}$. Our aim is to find the region at which $\chi(\kappa; \mathbf{w}_l^c) \le 0$. Note that

$$\chi'(\kappa; \mathbf{w}_q) = \frac{1}{\kappa^2}\frac{K_R}{K_L}\left(\frac{A_+}{A_0}\right)^{-m}\left[1 - \left(\frac{\kappa K_L}{K_R}\right)^{\frac{m}{m+2}}\left(\frac{A_+}{A_0}\right)^m\left(\frac{u_+}{c_+}\right)^{\frac{2m}{m+2}}\right]. \tag{3.37}$$

From definition of (3.31), we obtain that

$$c_+^2 = (c_l^c)^2\left(\frac{K}{K_L}\right)^{\frac{2}{m+2}}\left(\frac{c_+}{u_+}\right)^{\frac{2m}{m+2}}. \tag{3.38}$$

By (3.38), (3.37) can be simplified to

$$\chi'(\kappa; \mathbf{w}_q) = \frac{1}{\kappa^2}\frac{K_R}{K_L}\left(\frac{A_+}{A_0}\right)^{-m}\left[1 - \left(\frac{A_l^c}{A_0}\right)^m\left(\frac{K_L}{K_R}\right)^{\frac{m}{m+2}}\right]. \tag{3.39}$$

Due to (3.28) we get

$$(u_l^c)^2 = (c_l^c)^2 > \frac{\frac{2m}{\rho(m+2)}(K_R - K_L)}{\left(\frac{K_R}{K_L}\right)^{\frac{2}{m+2}} - 1}. \tag{3.40}$$

The definition of $c_l^c = c(A_l^c, K_L)$ in (2.1) implies that

$$\left(\frac{A_l^c}{A_0}\right)^m = \frac{\rho\,(c_l^c)^2}{mK_L}. \tag{3.41}$$

It follows that

$$\left(\frac{A_l^c}{A_0}\right)^m \left(\frac{K_L}{K_R}\right)^{\frac{m}{m+2}} = \frac{\rho\left(c_l^c\right)^2}{mK_L}\left(\frac{K_L}{K_R}\right)^{\frac{m}{m+2}}. \tag{3.42}$$

Taking (3.42) into (3.40) we obtain that

$$\left(\frac{A_l^c}{A_0}\right)^m \left(\frac{K_L}{K_R}\right)^{\frac{m}{m+2}} > \frac{\frac{2}{m+2}\left(\frac{K_R}{K_L}-1\right)}{\left(\frac{K_R}{K_L}\right)^{\frac{2}{m+2}}-1}\left(\frac{K_R}{K_L}\right)^{\frac{-m}{m+2}}. \tag{3.43}$$

Next we identify the inequality

$$\frac{\frac{2}{m+2}\left(\frac{K_R}{K_L}-1\right)}{\left(\frac{K_R}{K_L}\right)^{\frac{2}{m+2}}-1}\left(\frac{K_R}{K_L}\right)^{\frac{-m}{m+2}} > 1. \tag{3.44}$$

Set $x = \frac{K_R}{K_L}$. So $x < 1$ and (3.44) suggests to study the following function

$$D(x) := -\frac{m}{m+2}x^{\frac{2}{m+2}} - \frac{2}{m+2}x^{\frac{-m}{m+2}} + 1 < 0.$$

Note that

$$D'(x) = -\frac{2m}{(m+2)^2}x^{-\frac{m}{m+2}}(x-1) > 0 \qquad \text{when} \qquad x < 1.$$

So $D(x) < D(1) = 0$ when $x < 1$. Thus from (3.44), (3.43), and (3.39), we conclude that $\chi'(\kappa; \mathbf{w}_l^c) < 0$. Consequently it follows that

$$\chi(\kappa; \mathbf{w}_l^c) < \chi\left(\frac{K_R}{K_L}; \mathbf{w}_l^c\right) = \frac{m+2}{2m}\left(\frac{u_+}{c_+}\right)^{\frac{2m}{m+2}} - \frac{1}{2}\left(\frac{u_+}{c_+}\right)^2 - \frac{1}{m} < 0.$$

Thus the state $\mathbf{w} = \mathbf{J}(K_R; \mathbf{w}_+, K)$ always exists. This finishes the proof of the lemma. □

LEMMA 3.10. *We have*

$$\mathbf{J}(K_R; \mathbf{w}_l^c, K_L) = \mathbf{J}(K_R; \bar{\mathbf{w}}^{\kappa_c}, \kappa_c K_L), \tag{3.45}$$

*where* $\bar{\mathbf{w}}^{\kappa_c} = \mathbf{J}(\kappa_c K_L; \mathbf{w}_l^c, K_L)$ *and*

$$\kappa_c = \begin{cases} 1, & A_l^c \geq A_0, \\ \kappa_l^\tau, & A_l^c < A_0 \text{ and } A_0 \leq A_{s0s}^{l,c}. \end{cases}$$

*Proof.* From Lemma 3.9 we know that $\kappa_c \leq 1$. On one hand if $\kappa_c = 1$, then $\bar{\mathbf{w}}^{\kappa_c} = \mathbf{w}_l^c$, so (3.45) is trivial. On the other hand if $\kappa_c = \kappa_l^\tau < 1$, we have $\bar{\mathbf{w}}^{\kappa_c}$ is a critical state which satisfies

$$\bar{c}^{\kappa_c} = \bar{u}^{\kappa_c} = \kappa_c^{\frac{1}{m+2}} u_l^c. \tag{3.46}$$

Also from the definition of $\kappa_c$, we have $\tau(\kappa_c; \mathbf{w}_l^c) = 0$, i.e.

$$\frac{m+2}{2}\kappa_c^{\frac{2}{m+2}} = \frac{m+2}{2} + (\kappa_c - 1)\frac{mK_L}{\rho\left(u_l^c\right)^2}. \tag{3.47}$$

Considering the velocity function related to the stationary state $\mathbf{w} = \mathbf{J}(K_R; \bar{\mathbf{w}}^{\kappa_c}, \kappa_c K_L)$, we have

$$\begin{aligned}\phi(u; \bar{\mathbf{w}}^{\kappa_c}, \kappa_c K_L, K_R) &= \tfrac{1}{2}\rho u^2 + K_R\left[\tfrac{\rho}{m\kappa_c K_L}\tfrac{(\bar{u}^{\kappa_c})^{m+2}}{u^m} - 1\right] - \tfrac{1}{2}\rho\left(\bar{u}^{\kappa_c}\right)^2 \\ &\quad -\kappa_c K_L\left[\tfrac{\rho}{m\kappa_c K_L}\left(\bar{u}^{\kappa_c}\right)^2 - 1\right].\end{aligned} \tag{3.48}$$

Taking (3.46) into (3.48), we obtain that

$$\phi(u; \bar{\mathbf{w}}^{\kappa_c}, \kappa_c K_L, K_R) = \frac{1}{2}\rho u^2 + K_R\left[\frac{\rho}{mK_L}\frac{(u_l^c)^{m+2}}{u^m} - 1\right] - \frac{m+2}{2m}\rho\left(u_l^c\right)^2\kappa_c^{\frac{2}{m+2}} + \kappa_c K_L$$

Using (3.47), we have

$$\phi(u; \bar{\mathbf{w}}^{\kappa_c}, K_L, K_R) = \frac{1}{2}\rho u^2 + \frac{K_R}{K_L}\frac{\rho}{m}\frac{(u_l^c)^{m+2}}{u^m} - \frac{\rho(m+2)}{2m}\left(u_l^c\right)^2 + K_L - K_R. \tag{3.49}$$

This implies that the velocity function (3.49) of $\mathbf{J}(K_R; \bar{\mathbf{w}}^{\kappa_c}, K_L)$ is the same for $\bar{\mathbf{w}}_c = \mathbf{J}(K_R; \mathbf{w}_l^c, K_L)$. Hence (3.45) is true. □

REMARK 3.11. *For any subcritical state $\mathbf{w} \in P_{s0s}^j(\mathbf{w}_q^c)$, the components of $\mathbf{w} = (A, u)^T$ can be viewed as functions of $K$. Note that the transmural pressure $\Psi = \Psi(A, K_R)$ defined in (1.2) depends on $A$. By a length computation we obtain the relations*

$$\frac{d\Psi}{dK} = -\frac{m(\Psi + K_R)}{u}\frac{du}{dK}, \tag{3.50}$$

$$\frac{\rho}{u}(u^2 - c^2)\frac{du}{dK} = \frac{A_-}{A_+}\left(1 - \frac{A_-}{A_+}\right)\left(\frac{\rho u_-^2}{mK} - \frac{A_+}{A_-}\right). \tag{3.51}$$

*With the help of $u^2 - c^2 < 0$ and $A_- > A_+$ for $j = 1$, while $A_- < A_+$ for $j = 2$, we relate the monotonicity of $P_{s0s}^j(\mathbf{w}_q^c)$ to the sign of $\frac{\rho u_-^2}{mK} - \frac{A_+}{A_-}$. Specifically we have*

$$\frac{1}{u}\frac{du}{dK} < 0 \text{ if } \quad \frac{\rho u_-^2}{mK} - \frac{A_+}{A_-} > 0, \tag{3.52}$$

*while*

$$\frac{1}{u}\frac{du}{dK} > 0 \text{ if } \quad \frac{\rho u_-^2}{mK} - \frac{A_+}{A_-} > 0. \tag{3.53}$$

*The detailed derivation of this remark will be found in [12, p.13-14 ]. The conditions in this remark are satisfied under the conjecture given in [12, Assumption 3.15].*

**3.2. The classification of L–M and R–M curves for $K_L > K_R$.** According to Lemmas 3.4, 3.7, and 3.9, for the subcritical initial Riemann data under the assumption $K_L > K_R$, we can classify the L–M and R–M curves into three and two different cases respectively. They are given in Table 3.1. We point out that Case $VI_l$ of the L–M curve is named to keep the consistency of notation of cases defined for the R–M curves. Note that the local speed index variable $S_{L,R}^I = |\frac{u_{L,R}}{c_{L,R}}| \le 1$ in Cases $I_{l,r}$, $II_{l,r}$. But the local speed index variable $S_L^I$ of the initial state $\mathbf{w}_L$ is not determined in Case $VI_l$. It could be subcritical or supercritical. In the following sections each case of the L–M curve will be studied. The R–M curve can be treated likewise.

TABLE 3.1
*Cases of L–M and R–M curves*

| Cases | | Cases | |
|---|---|---|---|
| $I_l$: | $A^{P^1_{ES}}_{max} \geq A_0 \left[1 - \frac{K_R}{K_L}\right]^{\frac{1}{m}}$; $u_L \leq c_L$; $u_l^c \leq u_l^{sc}$ | $I_r$: | $u_R + c_R \geq 0$; $u_r^c < -u_r^{sc}$ |
| $II_l$: | $A^{P^1_{ES}}_{max} \geq A_0 \left[1 - \frac{K_R}{K_L}\right]^{\frac{1}{m}}$; $u_L \leq c_L$; $u_l^c > u_l^{sc}$ | $II_r$: | $u_R + c_R \geq 0$; $u_r^c \geq -u_r^{sc}$ |
| $VI_l$: | $A^{P^1_{ES}}_{max} < A_0 \left[1 - \frac{K_R}{K_L}\right]^{\frac{1}{m}}$ | | |

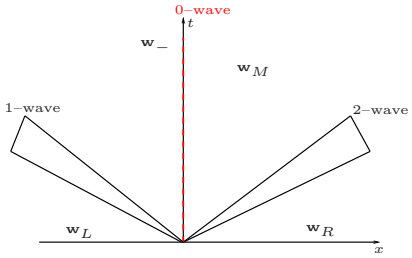


FIG. 3.1. *Wave configuration A*

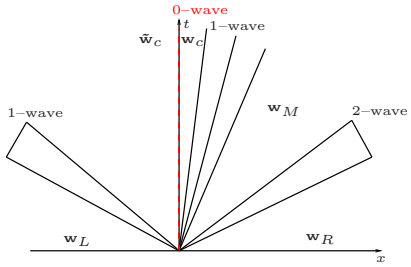


FIG. 3.2. *Wave configuration B*

**3.3. Cases of L–M curves.** In this section we construct the L–M curve for all possible cases with a subcritical initial state. The construction is validated by a series of examples. Unless otherwise stated, the computational region for the Riemann problem is $]0, 1[$. The equilibrium cross sectional area is $A_0 = 2.1124 \times 10^{-4}$. The discontinuity is located at $x = 0.5$.

**3.3.1. Case $I_l$: $A^{P^1_{ES}}_{max} \geq A_0 \left[1 - \frac{K_R}{K_L}\right]^{\frac{1}{m}}$, $u_L \leq c_L$ and $u_l^c \leq u_l^{sc}$.** In this case the possible wave configurations with positive intermediate velocity are the wave configurations $A$ and $B$, see Figures 3.1 and 3.2. The wave configuration $A$ is classical. It consists of, from left to right, a 1–wave, a stationary wave located at $x = 0$, and a 2–wave. The wave configuration $B$ consists of, from left to right, a resonant wave due to the fact that the stationary wave coincides with the 1–wave, and a 2–wave. The 1–wave, in such a case, is definitely a transcritical rarefaction wave because the 1–shock has a negative speed due to the Lax entropy condition (2.6). Therefore, the resonant wave here is constituted of two parts, the first part is a 1–wave along $T_1(\mathbf{w}_L)$ from the state $\mathbf{w}_L$ to the state $\tilde{\mathbf{w}}_c$; the second part is the 1–wave along $T_1(\mathbf{w}_c)$. These two parts are separated by a stationary wave $\mathbf{w}^c = \mathbf{J}(K_R; \tilde{\mathbf{w}}^c, K_L)$, where $\tilde{\mathbf{w}}^c \in T_1(\mathbf{w}_L)$ and $\mathbf{w}^c$ is a critical state. Specifically, the state $\tilde{\mathbf{w}}^c = (\tilde{A}^c, \tilde{u}^c)$ is subcritical, and $\tilde{A}^c$ is the solution to $\Omega_l(A; \mathbf{w}_L, K_L, K_R) = 0$ while $\tilde{u}_c = u_L - f_L(\tilde{A}_c; \mathbf{w}_L)$. We use an iteration method to calculate it.

Consequently the L–M curve $C_L(\mathbf{w}_L)$ consists of three parts

$$
\begin{aligned}
&P_1^l(\mathbf{w}_L) = \{\mathbf{w} | \mathbf{w} \in T_1(\mathbf{w}_L) \text{ with } u \leq 0\}, \\
&P_2^l(\mathbf{w}_L) = \{\mathbf{w} | \mathbf{w} = \mathbf{J}(K_R; \mathbf{w}_-, K_L) \text{ and } \mathbf{w}_- \in T_1(\mathbf{w}_L) \text{ with } 0 < u < u^c\}, \\
&P_3^l(\mathbf{w}_L) = \{\mathbf{w} | \mathbf{w} \in T_1(\mathbf{w}^c) \text{ with } u > u^c\}.
\end{aligned}
$$

Note that $P_1^l(\mathbf{w}_L)$ and $P_3^1(\mathbf{w}_L)$ are parts of $T_1(\mathbf{w}_L)$ and $T_1(\mathbf{w}^c)$ respectively; While $P_2^l(\mathbf{w}_L) = P_{ES}^1(\mathbf{w}_L)$. Therefore, according to Lemmas 2.1 and 3.8, the L–M curve

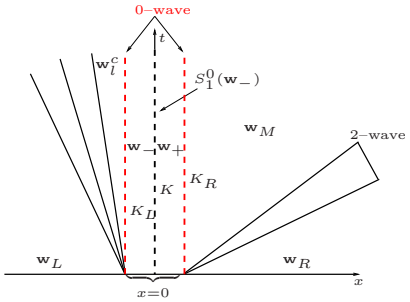


FIG. 3.3. *Wave configuration C*

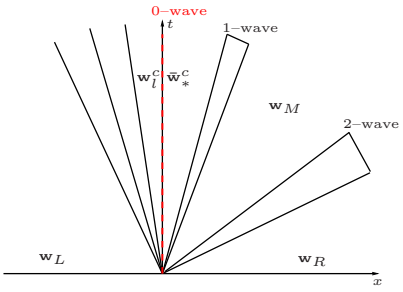


FIG. 3.4. *Wave configuration D*

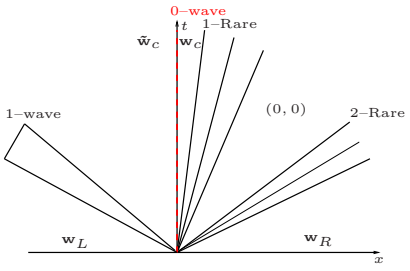


FIG. 3.5. *Wave configuration $B_{col}$*

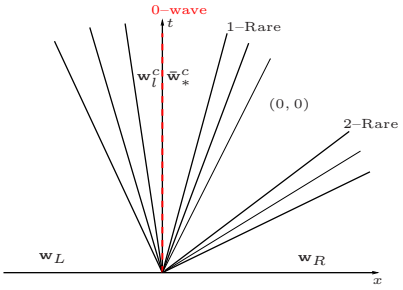


FIG. 3.6. *Wave configuration $D_{col}$*

$\bigcup_{j=1}^{3} P_j^l(\mathbf{w}_L)$ in this case is strictly decreasing in the $(u, \Psi)$ state plane. We define a critical velocity which is related to the collapse state on the L–M curve in this case, i.e.

$$u_{col}^{LM} = \frac{m+2}{m} u^c. \tag{3.54}$$

Note that if $u_{col}^{LM} > u_{col}^{R}$, then there exists one unique intersection point between the L–M and R–M curves. This intersection point is one of the intermediate states of the Riemann solution. We use $\mathbf{w}_M$ determine it. This implies that in such kind of the case, the Riemann solution uniquely exists. Moreover if $\mathbf{w}_M \in P_2^l(\mathbf{w}_L)$, the exact Riemann solution has the wave configuration A. While if the intermediate state $\mathbf{w}_M \in P_3^l(\mathbf{w}_L)$, the exact Riemann solution has the wave configuration B.

Two examples are used to illustrate our construction. To preserve the continuity, all the states on the L–M curve are projected into the $(u, \Psi)$ state plane. The first example in Table 3.2 is related to the wave configuration A. It was first proposed by Toro and Siviglia in [32]. The corresponding L–M curve, the exact Riemann solution

TABLE 3.2
*An example with the wave configuration A in Case $II_l$ by Toro and Siviglia [32]*

| | $K$ $(Pa)$ | $A$ $(m^2)$ | $u$ $(m/s)$ | $S^I$ |
|---|---|---|---|---|
| $\mathbf{w}_L$ | 2000003.266554 | $3.0 \times 10^{-4}$ | $-2.6575 \times 10^{-5}$ | $-7.88826 \times 10^{-7}$ |
| $\mathbf{w}_-$ | 2000003.26654 | $2.01185 \times 10^{-4}$ | 12.81037 | 0.420195 |
| $\mathbf{w}_M$ | 40000.06533 | $6.34034 \times 10^{-4}$ | 4.0648486 | 0.107114 |
| $\mathbf{w}_R$ | 40000.06533 | $3 \times 10^{-4}$ | $6.123 \times 10^{-6}$ | $1.28516 \times 10^{-6}$ |

of the blood vessel as well as velocity are shown in Figure 3.7.

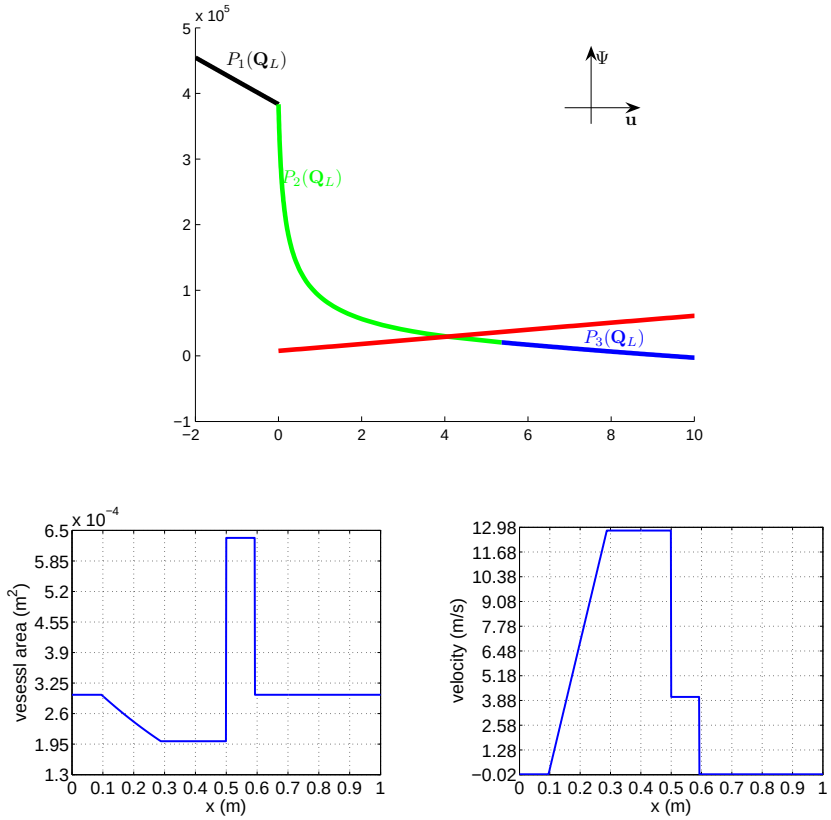


FIG. 3.7. *Top: L–M curve* $\bigcup_{k=1}^{3} P_k(\mathbf{w}_L)$ *for Table 3.2. Bottom: the corresponding exact vessel area and velocity at* $t = 0.012$ *s.*

The second example is related to the wave configuration B. The Riemann initial data and the states of the exact Riemann solution are shown in Table 3.3. The L–M curve and the exact solution are shown in Figure 3.8.

TABLE 3.3
*An example with the wave configuration B in Case* $I_l$

| | $K\ (Pa)$ | $A\ (m^2)$ | $u\ (m/s)$ | $S^I$ |
|---|---|---|---|---|
| $\mathbf{w}_L$ | 2000003.266554 | $3.0 \times 10^{-4}$ | $-2.6575 \times 10^{-5}$ | $-7.88826 \times 10^{-7}$ |
| $\tilde{\mathbf{w}}_c$ | 2000003.26654 | $2.0034 \times 10^{-4}$ | 12.938557 | 0.424847 |
| $\mathbf{w}_c$ | 40000.06533 | $4.82994 \times 10^{-4}$ | 5.36675 | 1 |
| $\mathbf{w}_M$ | 40000.06533 | $4.13503 \times 10^{-4}$ | 6.18445 | 1.197995 |
| $\mathbf{w}_R$ | 40000.06533 | $1.17 \times 10^{-4}$ | $1.5 \times 10^{-7}$ | $3.984 \times 10^{-8}$ |

On the other hand if $u_{col}^{LM} \leq u_{col}^{R}$, then the L–M and R–M curves intersect the line $\Psi = -K_R$, i.e. $A = 0$ before they meet each other. Hence the corresponding Riemann solution contains a collapsible vessel state with the wave configuration $B_{col}$,

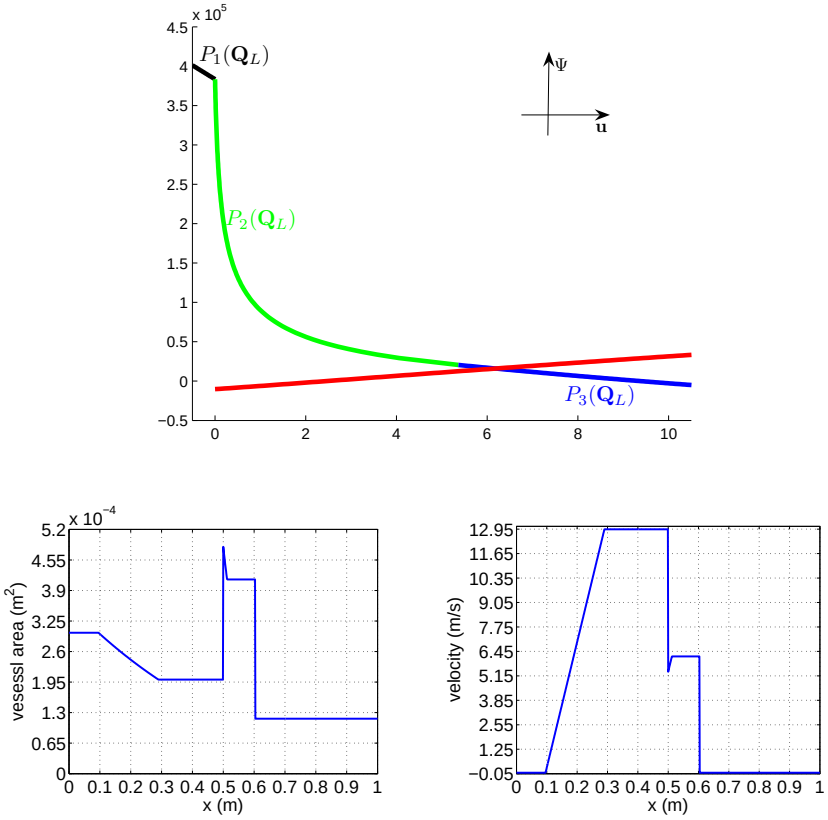


FIG. 3.8. *Top:L–M curve* $\bigcup_{k=1}^{3} P_k(\mathbf{w}_L)$ *for Table 3.3. Bottom: the corresponding exact vessel area and velocity at* $t = 0.012$ *s.*

see Figure 3.5. Table 3.4 gives an example with the initial and intermediate states. Figure 3.9 presents the corresponding blood vessel cross sectional area and velocity.

TABLE 3.4
*An example with the wave configuration* $B_{col}$ *in Case* $I_l$

| | $K\ (Pa)$ | $A\ (m^2)$ | $u\ (m/s)$ | $S^I$ |
|---|---|---|---|---|
| $\mathbf{w}_L$ | 2000003.266554 | $3.0 \times 10^{-4}$ | $-2.675 \times 10^{-5}$ | $-7.88826 \times 10^{-7}$ |
| $\tilde{\mathbf{w}}_c$ | 2000003.26654 | $1.89 \times 10^{-4}$ | 14.7104757 | 0.029343 |
| $\mathbf{w}_c$ | 2000.003267 | $1.693 \times 10^{-3}$ | 1.641941 | 1 |
| $\mathbf{w}_{col}^{LM}$ | 2000.003267 | 0 | 8.209704 | not defined |
| $\mathbf{w}_{col}^{R}$ | 2000.003267 | 0 | 11.632418 | not defined |
| $\mathbf{w}_R$ | 2000.003267 | $1.17e-4$ | 15 | 17.81694 |

**3.3.2. Case** $II_l$**:** $A_{max}^{P_{ES}^1} \geq A_0 \left[1 - \frac{K_R}{K_L}\right]^{\frac{1}{m}}$**,** $u_L \leq c_L$**, and** $u_l^c > u_l^{sc}$**.** In this case the possible wave configurations with positive intermediate velocity are the wave configurations $A$, $C$, and $D$, see Figures 3.1, 3.3 and 3.4. The wave configuration $A$ is the same as the one in Case $I_l$. The wave configuration $C$ consists of, from left to

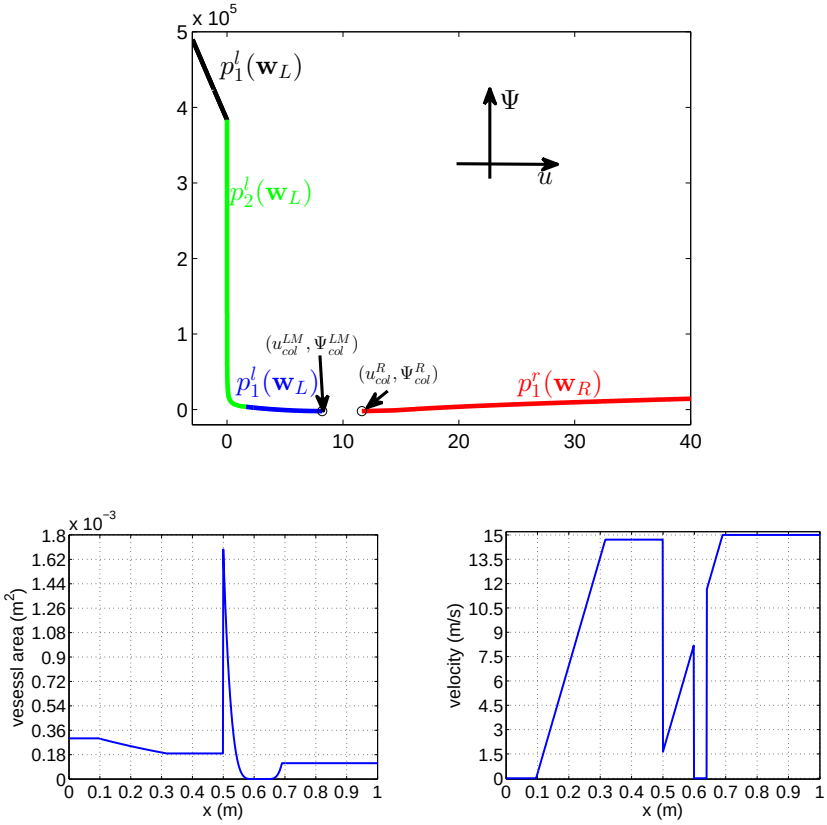


FIG. 3.9. *Top:L–M curve* $\bigcup_{k=1}^{3} P_k(\mathbf{w}_L)$ *for Table 3.3, where* $\Psi_{col}^L = \Psi_{col}^R = -K_R$. *Bottom: the corresponding exact vessel area and velocity at* $t = 0.012$ *s.*

right, a resonant wave due to the coincidence of stationary wave with the transcritical rarefaction, and a 2–wave. The resonant wave in the wave configuration $C$ is constituted of a rarefaction wave along $T_1(\mathbf{w}_L)$ fanning from the state $\mathbf{w}_L$ to the critical state $\mathbf{w}_l^c = (A_l^c, u_l^c)^T$ which are defined in (3.9) and (3.10), followed by a succession of three waves: a supercritical stationary wave $\mathbf{w}_- = \mathbf{J}(K; \mathbf{w}_l^c, K_L)$, a 0–speed 1–shock wave $\mathbf{w}_+ = S_1^0(\mathbf{w}_-)$ and a subcritical stationary wave $\mathbf{w} = \mathbf{J}(K_R; \mathbf{w}_+, K)$, where $K \in ]K_l,\ K_r[$ defined in (3.32). All of the three waves coalesce on the line $x = 0$. The wave configuration $D$ consists of, from left to right, a resonant wave and a 2–wave. The resonant wave in the wave configuration $D$ has two parts, the first part is a rarefaction wave along $T_1(\mathbf{w}_L)$ from the state $\mathbf{w}_L$ to the critical state $\mathbf{w}_l^c$; the second part is a 1–wave along $T_1(\bar{\mathbf{w}}_*^c)$, where $\bar{\mathbf{w}}_*^c$ represents a supercritical state of $\mathbf{J}(K_R; \mathbf{w}_l^c, K_L)$.

Consequently the L–M curve $C_L(\mathbf{w}_L)$ consists of four following parts:

$$
\begin{aligned}
&P_1^l(\mathbf{w}_L) = \{\mathbf{w} | \mathbf{w} \in T_1(\mathbf{w}_L) \text{ with } u < 0\}\,,\\
&P_2^l(\mathbf{w}_L) = \{\mathbf{w} | \mathbf{w} = \mathbf{J}(K_R; \mathbf{w}_-, K_L) \text{ and } \mathbf{w}_- \in T_1(\mathbf{w}_L) \text{ with } 0 < u < \bar{u}^c\}\,,\\
&P_3^l(\mathbf{w}_L) = \{\mathbf{w} | \mathbf{w} = \mathbf{J}(K_R; \mathbf{w}_+, K);\ \mathbf{w}_+ = S_1^0(\mathbf{w}_-);\ \mathbf{w}_- = \mathbf{J}(K; \mathbf{w}_l^c, K_L),\ K_l \le K \le K_r\}\,,\\
&P_4^l(\mathbf{w}_L) = \left\{\mathbf{w} | \mathbf{w} \in T_1(\bar{\mathbf{w}}_*^c) \text{ with } u > \hat{\bar{u}}^c\right\}\,,
\end{aligned}
$$

where $\hat{\bar{\mathbf{w}}}^c = S_1^0(\bar{\mathbf{w}}_*^c)$. As we have mentioned in Remark 2.4, the stationary wave $\mathbf{J}(K_R;\mathbf{w}_l^c,K_L)$ has two solutions. One is subcritical and the other is supercritical. We use $\bar{\mathbf{w}}^c = \mathbf{J}(K_R;\mathbf{w}_l^c,K_L)$ and $\bar{\mathbf{w}}_*^c = \mathbf{J}(K_R;\mathbf{w}_l^c,K_L)$ to denote the subcritical one and the supercritical one respectively. Hence the segment $P_2^l(\mathbf{w}_L)$ ends at the subcritical state $\bar{\mathbf{w}}^c$. According to Lemma 3.10 the left boundary of $P_3^l(\mathbf{w}_L)$ is also $\bar{\mathbf{w}}^c$. So we establish the continuity of L–M curve in this case.

Note that $P_3^l(\mathbf{w}_L) = P_{s0s}^1(\mathbf{w}_l^c)$. Due to (3.51) we have to consider the sign of $\frac{\rho u_-^2}{mK} - \frac{A_+}{A_-}$ when $K$ varies from $K_l$ to $K_r$. We take $K = K_r$ as an example. From the definition (3.32), there are three different cases.

The first case is for $A_l^c \geq A_0$ and $K_r = K_L$. Therefore $\frac{\rho u_-^2}{mK} - \frac{A_+}{A_-}$ at $K = K_L$ is

$$\frac{\rho\left(u_l^c\right)^2}{mK_L} - 1 = \left(\frac{A_l^c}{A_0}\right)^m - 1 \geq 0. \tag{3.55}$$

The second case is for $A_l^c < A_0$ and $K_r = \kappa_l^\tau K_L$, where $\kappa_l^\tau < 1$ is the solution to $\tau(\kappa;\mathbf{w}_l^c) = 0$ in (3.33). The details of $\kappa_l^\tau$ can be found in Lemma 3.9. We use $\bar{\mathbf{w}}_{\kappa_l^\tau}^c$ to denote the state $\mathbf{J}(\kappa_l^\tau K_L;\mathbf{w}_l^c,K_L)$. With (3.46) the relation $\frac{\rho u_-^2}{mK} - \frac{A_+}{A_-}$ at $\kappa_l^\tau K_L$ becomes

$$\frac{\rho\left(\bar{u}_{\kappa_l^\tau}^c\right)^2}{m\kappa_l^\tau K_L} - 1 = \frac{\rho\left(\kappa_l^\tau\right)^{\frac{2}{m+2}}\left(\bar{u}_l^c\right)^2}{m\kappa_l^\tau K_L} - 1 = \left(\kappa_l^\tau\right)^{-\frac{m}{m+2}}\left(\frac{A_l^c}{A_0}\right)^m - 1. \tag{3.56}$$

From (3.47), we obtain that

$$\left(\kappa_l^\tau\right)^{-\frac{m}{m+2}}\left(\frac{A_l^c}{A_0}\right)^m = \frac{\frac{2}{m+2}\left(\kappa_l^\tau - 1\right)}{\left(\kappa_l^\tau\right)^{\frac{m}{m+2}}\left[\left(\kappa_l^\tau\right)^{\frac{2}{m+2}} - 1\right]}. \tag{3.57}$$

Inserting (3.57) into (3.56), we get

$$\frac{\rho\left(\bar{u}_{\kappa_l^\tau}^c\right)^2}{m\kappa_l^\tau K_L} - 1 = \frac{-\frac{m}{m+2}\kappa_l^\tau + \left(\kappa_l^\tau\right)^{\frac{m}{m+2}} - \frac{2}{m+2}}{\left(\kappa_l^\tau\right)^{\frac{m}{m+2}}\left[\left(\kappa_l^\tau\right)^{\frac{2}{m+2}} - 1\right]} > 0 \qquad \text{due to} \qquad \kappa_l^\tau < 1. \tag{3.58}$$

Consequently for the first and second cases, with (3.52) we have $\frac{du}{dK} < 0$ since $u > 0$. Note that $\frac{d\Psi}{dK} = -\frac{1}{K_R u}\frac{du}{dK} > 0$. Thus $\frac{d\Psi}{du} = \frac{\frac{d\Psi}{dK}}{\frac{du}{dK}} < 0$. Hence the segment $P_3^l(\mathbf{w}_L)$ is continuously decreasing on the $(u,\Psi)$ state plane.

The third case is for $K_l = K_r = K_L$, i.e. the segment $P_{s0s}^1(\mathbf{w}_l^c)$ degenerates into a point which is also the boundary of the segment $P_2(\mathbf{w}_L)$. Thus the segment of $P_3^l(\mathbf{w}_L)$ in this case is trivial.

On the whole, analogously to Case $I_l$, the L–M curve $\bigcup_{j=1}^{4} P_j^l(\mathbf{w}_L)$ in this case is strictly decreasing in the $(u,\Psi)$ plane. We use

$$u_{col}^{LM} = \bar{u}_*^c + \frac{2}{m}\bar{c}_*^c \tag{3.59}$$

to denote the critical velocity which is related to collapsible vessels on the L–M curve. Note that if $u_{col}^{LM} > u_{col}^R$, there exists one unique intersection point of the L–M and

R–M curves. This intersection point is one of intermediate state of the corresponding Riemann solution. It implies that the exact Riemann solution uniquely exists. Moreover if the intermediate state $\mathbf{w}_M \in P_2^l(\mathbf{w}_L)$, the exact Riemann solution has the wave configuration A. While if the intermediate state $\mathbf{w}_M \in P_3^l(\mathbf{w}_L)$, the exact Riemann solution has the wave configuration C. And if the intermediate state $\mathbf{w}_M \in P_4^l(\mathbf{w}_L)$, the exact Riemann solution has the wave configuration D.

Two examples are used here to show the corresponding exact Riemann solutions with the wave configurations $C$ and $D$ respectively. The Riemann initial data and states of the exact solution to the first example with the wave configuration $C$ are listed in Table 3.5. The corresponding L–M curve and the exact Riemann solutions are shown in Figure 3.10. We cannot observe the resonant wave due to the fact that two stationary waves and zero speed 1–shock coalesce on the line $x = 0$. The Riemann initial data and the states of the exact solution to the second example with the wave configuration $D$ are listed in Table 3.6. The corresponding L–M curve and the exact Riemann solution are shown in Figure 3.11.

TABLE 3.5
*An example with the wave configuration C for Case $II_l$*

| | $K\ (Pa)$ | $A\ (m^2)$ | $u\ (m/s)$ | $S^I$ |
|---|---|---|---|---|
| $\mathbf{w}_L$ | 2000003.26654 | $6.0 \times 10^{-4}$ | $2.6575 \times 10^{-5}$ | $6.63321 \times 10^{-7}$ |
| $\mathbf{w}_c^l$ | 2000003.26654 | $2.4576 \times 10^{-4}$ | 32.050849 | 1 |
| $\mathbf{w}_-$ | 59436.680223 | $2.16361 \times 10^{-4}$ | 36.405913 | 6.802265 |
| $\mathbf{w}_+$ | 59436.680223 | $3.539357 \times 10^{-4}$ | 2.225495 | 0.206763 |
| $\mathbf{w}_M$ | 40000.06533 | 0.006727565 | 1.170828 | 0.112928 |
| $\mathbf{w}_R$ | 40000.06533 | 0.006 | 0 | 0 |

TABLE 3.6
*The Riemann initial data and intermediate states of the wave configuration D for Case $II_l$*

| | $K\ (Pa)$ | $A\ (m^2)$ | $u\ (m/s)$ | $S^I$ |
|---|---|---|---|---|
| $\mathbf{w}_L$ | 2000003.26654 | $6.0 \times 10^{-4}$ | $2.6575 \times 10^{-5}$ | $6.63321 \times 10^{-7}$ |
| $\mathbf{w}_l^c$ | 2000003.26654 | $2.4576 \times 10^{-4}$ | 32.05085 | 1 |
| $\bar{\mathbf{w}}_*^c$ | 40000.06533 | $2.16324 \times 10^{-4}$ | 36.412129 | 8.293602 |
| $\mathbf{w}_M$ | 40000.06533 | 0.003946778 | 5.84423 | 0.64408 |
| $\mathbf{w}_R$ | 40000.06533 | 0.002 | 0 | 0 |

On the other hand if $u_{col}^{LM} < u_{col}^R$, analogously to Case $I_l$, the L–M and R–M curves have no intersection point. The corresponding Riemann solution contains a collapsible vessel state with the wave configuration $D_{col}$, see Figure 3.6. Table 3.7 gives the Riemann initial data and the intermediates states of an example. The corresponding vessel area and the velocity are shown in Figure 3.12. We can clearly observe the tube collapsible states in the right part of the solutions.

**3.3.3. Case $VI_l$: $A_{max}^{P_{ES}^1} < A_0 \left[1 - \frac{K_R}{K_L}\right]^{\frac{1}{m}}$.** This is a very special case which contains the backflow and the blood vessel collapse problem. Mathematically it is due to the fact that the basic wave curve $P_{ES}^1(\mathbf{w}_L)$ fails to exist. The details can be found in Section 3.1.2. The necessary conditions for this case are $u_{col}^R > 0$ and $u_{col}^L > 0$. The corresponding Riemann solution has the wave configuration $A_{col}^2$, see Figure 3.14. It contains a 1–wave, a 2–rarefaction, but no stationary waves, since it

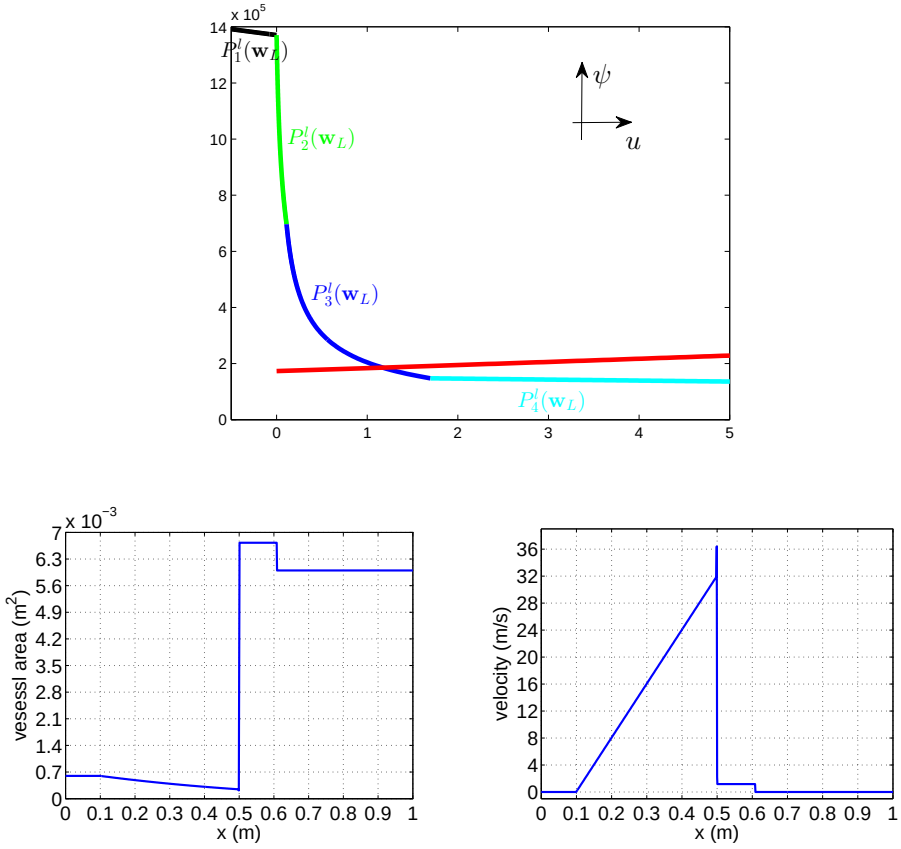


FIG. 3.10. *Top: L–M curve* $\bigcup_{k=1}^{4} P_k(\mathbf{w}_L)$ *for Table 3.5. Bottom: the corresponding exact vessel area and velocity at* $t = 0.01$ *s.*

TABLE 3.7
*The Riemann initial data and intermediate states of the wave configuration* $D_{col}$ *for Case* $II_l$

| | $K$ $(Pa)$ | $A$ $(m^2)$ | $u$ $(m/s)$ | $S^I$ |
|---|---|---|---|---|
| $\mathbf{w}_L$ | 200.000327 | 0.08 | 1.089116 | 0.8 |
| $\mathbf{w}_l^c$ | 200.000327 | 0.067948 | 1.306939 | 1 |
| $\bar{\mathbf{w}}_*^c$ | 2.000003 | 0.03117 | 2.849041 | 26.488297 |
| $\mathbf{w}_{col}^{LM}$ | 2.000003 | 0 | 3.279274 | not defined |
| $\mathbf{w}_{col}^{R}$ | 2.000003 | 0 | 8.283464 | not defined |
| $\mathbf{w}_R$ | 2.000003 | 0.002 | 8.5 | 157.018116 |

fails to exist. The 1–wave in the wave configuration $A_{col}^2$ corresponds to the backflow of blood from the left initial state. The state $\mathbf{w}_M$ is the intermediate state of the Riemann solution with the following data

$$(K, A, u) = \begin{cases} (K_L, A_L, u_L), & x < 0, \\ (K_L, A_L, -u_L), & x > 0. \end{cases} \tag{3.60}$$

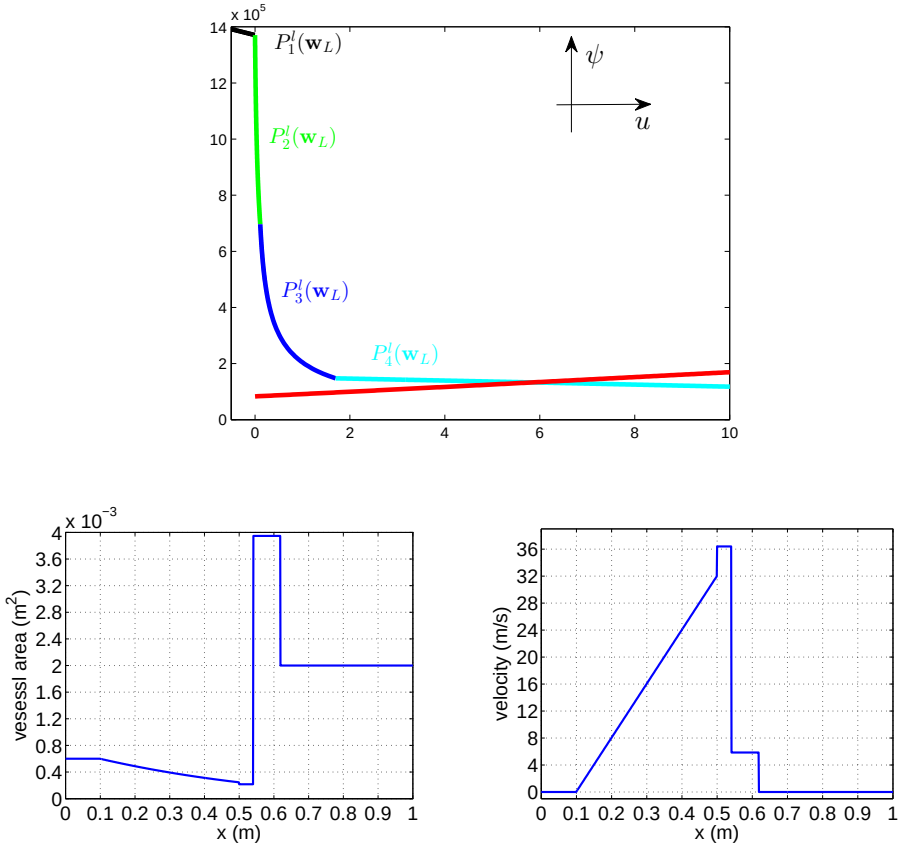


FIG. 3.11. *Top:L–M curve* $\bigcup_{k=1}^{4} P_k(\mathbf{w}_L)$ *for Table 3.6. Bottom: the corresponding exact vessel area and velocity at* $t = 0.01$ *s.*

TABLE 3.8
*The Riemann initial data and intermediate states of the wave configuration* $A^2_{col}$ *for Case VI*

| | $K$ $(Pa)$ | $A$ $(m^2)$ | $u$ $(m/s)$ | $S^I$ |
|---|---|---|---|---|
| $\mathbf{w}_L$ | 2000003.266554 | 0.0003 | $-13.0$ | $-0.385879$ |
| $\mathbf{w}_M$ | 2000003.266554 | 0.0002 | 0 | 0 |
| $\mathbf{w}_R$ | 40000.065331 | 0.0003 | 25.0 | 5.247265 |

We use an example in Table 3.8 to illustrate the solution with the wave configuration $A^2_{col}$. The corresponding blood vessel cross sectional area and the velocity are shown in Figure 3.15.

**3.4. Cases of R–M curves.** The R–M curve has two different cases for the subcritical initial Riemann data, see Table 3.1. The Riemann solutions related to the R–M curve have negative intermediate velocity. The corresponding wave configurations can be treated as appropriate symmetric cases of the ones with the positive velocity. For the sake of simplicity, we use the letters $A^T$, $B^T$, $B^T_{col}$, $C^T$, $D^T$ and $D^T_{col}$ to denote them. Note that the Case $I_r$ of the R–M curve is similar to the Case

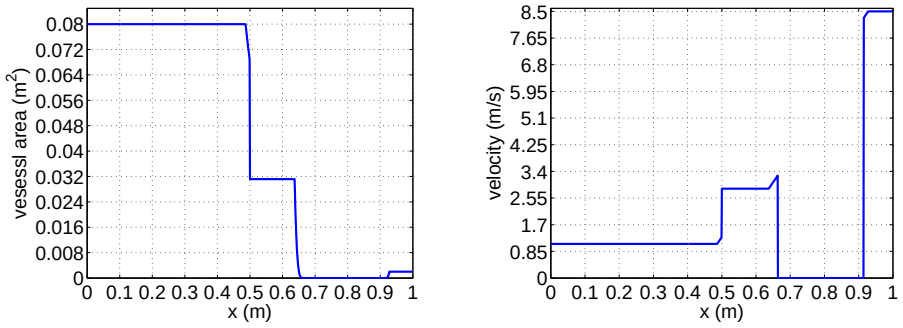


FIG. 3.12. *The exact vessel area and velocity at $t = 0.05$ s for Table 3.7.*

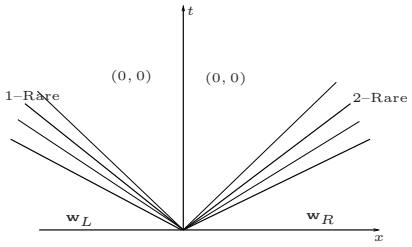


FIG. 3.13. *Wave configuration $A^1_{col}$*

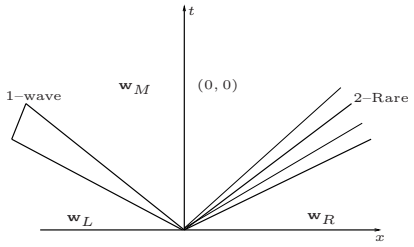


FIG. 3.14. *Wave configuration $A^2_{col}$*

$I_l$, while the Case $II_r$ of the R–M curve is similar to the Case $II_l$. All Cases of the R–M curves can be treated likewise the ones of the L–M curves, for example, we can use $P^r_j(\mathbf{w}_R)$, $j = 1, 2, 3, 4$ to denote the segments of R–M curve. Specifically the segment $P^r_1(\mathbf{w}_R)$ is common to all cases and defined in (3.6). Furthermore we have the segment $P^r_2(\mathbf{w}_R) = P^2_{ES}(\mathbf{w}_R)$. The existence and monotonicity of $P^r_2(\mathbf{w}_R)$ have been determined by Lemma 3.7 and 3.8. For the remaining of the segments, their definition depend on the cases. We just emphasize the following points.

In Case $I_r$, the R–M curve consists of three segments. The segment $P^r_3(\mathbf{w}_R) = T_2(\mathbf{w}^c)$, where $\mathbf{w}^c = \mathbf{J}(K_L; \tilde{\mathbf{w}}^c, K_R)$, and $\tilde{\mathbf{w}}^c \in T_2(\mathbf{w}_R)$. The blood vessel cross sectional area $\tilde{A}^c$ is the solution to $\Omega_r(A; \mathbf{w}_R, K_R, K_L) = 0$ while $\tilde{u}^c = u_R + f(\tilde{A}^c; \mathbf{w}_R)$. We use an iteration method to calculate it. Moreover, the critical velocity for the collapsible states is defined as

$$u^{RM}_{col} = \frac{m+2}{m} u_c. \tag{3.61}$$

So if $u^{RM}_{col} > u^L_{col}$, there is no intersection point between the L–M and R–M curves. The Riemann solution has the wave configuration $B^T_{col}$. Otherwise there is one unique solution located on the R–M curve. It might have the wave configuration $A^T$ or $B^T$.

In Case $II_r$, the R–M curve consists of four segments. The segment $P^r_3(\mathbf{w}_R) = P^2_{s0s}(\mathbf{w}^c_r)$ which has been extensively studied in Section 3.1.4. And we have the segment $P^r_4(\mathbf{w}_R) = T_2(\bar{\mathbf{w}}^c_*)$, where $\bar{\mathbf{w}}^c_*$ is a supercritical outflow state of the stationary wave $\mathbf{J}(K_L; \mathbf{w}^c_r, K_R)$. In addition the critical velocity for the collapsible vessel states in Case $II_r$ is defined as

$$u^{RM}_{col} = \bar{u}^c_* - \frac{2}{m}\bar{c}^c_*. \tag{3.62}$$

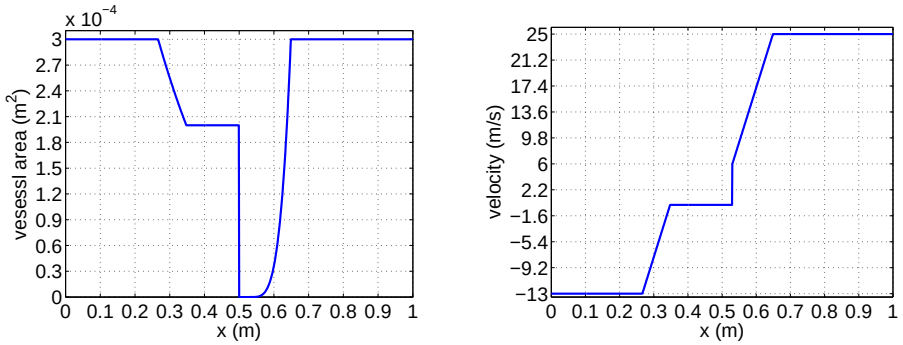


FIG. 3.15. *The exact vessel area and velocity at* $t = 0.005$ *s for Table 3.8.*

If $u_{col}^{RM} > u_{col}^{L}$, the Riemann solution has the wave configuration $D_{col}^{T}$. Otherwise it might have the wave configuration $A^T$, $C^T$ or $D^T$.

According to Lemmas 2.1 and 3.8, as well as the condition (3.51), the R–M curve in Cases $I_r$ and $II_r$ are continuous and increasing. So the Riemann solution is unique for the subcritical initial data $\mathbf{w}_R$. We can conclude that the Riemann solutions related to the R–M curve can be treated likewise the ones related to the L–M curve. It is not necessary to give them in detail.

**3.5. An algorithm for the exact Riemann solutions.** In this section we present a procedure for solving the Riemann problem (1.1) and (2.3) exactly. To find all possible exact Riemann solutions we need to introduce additional cases that contain the collapsible vessel states. The common point of the Riemann solutions with collapsible states in Section 3 is that these collapsible states arise due to the motion of the blood flow. Of course there also exists the interesting possibility that the left or right initial states are collapsed, i.e. $(A_L, u_L) = (0, 0)$ or $(A_R, u_R) = (0, 0)$. We use $(A_R, u_R) = (0, 0)$ to illustrate the solutions in such kind of the situation. First the corresponding L–M curve will still be defined as in Section 3.2. Then the Riemann solution might have the wave configurations $A_{col}^2$, $B_{col}$ and $D_{col}$. It completely depends on the left initial data. But we have to address the fact that the 2–rarefaction wave is entirely canceled in them.

From the previous discussion, in the context of the general cases we know that one of intermediate states of the exact Riemann solutions is the intersection point of the corresponding L–M and R–M curves. Here we have to keep in mind that the L–M curve degenerates into the 1–wave curve when the velocity is negative; while the R–M curve degenerates into the 2–wave curve when the velocity is positive. As we have already mentioned in the beginning of this section, the location of the stationary wave depends on the sign of the intermediate velocity. To determine it, we define two critical variables given as

$$\Psi_l = \Psi(A_{max}^{P_{ES}^1}, K_L), \quad \Psi_r = \Psi(A_{max}^{P_{ES}^2}, K_R), \tag{3.63}$$

where $A_{max}^{P_{ES}^1}$ and $A_{max}^{P_{ES}^2}$ are defined in (3.11) and (3.15) respectively. It can be easy proved that if $\Psi_l > \Psi_r$ the corresponding Riemann solution has a positive intermediate velocity. The stationary wave is located on the L–M curve. On the contrary if $\Psi_l > \Psi_r$ the corresponding Riemann solution has a negative intermediate velocity. The stationary wave is located on the R–M curve. One special case is when $\Psi_l = \Psi_r$.

In such kind of case the stationary wave is trivial with zero velocity. The corresponding Riemann solution has the wave configuration $A$, but with zero intermediate velocity.

Once the location of the stationary wave is determined, the L–M and R–M curves can be classified according to the given initial data. The details for the subcritical initial data can be found in Table 3.1. Here we address that the subcritical condition is only required for one of the states $\mathbf{w}_L$ and $\mathbf{w}_R$. From Cases $I_l$ and $II_l$, we know that the intersection point of the L–M and R–M curves corresponds to solving an algebraic system. It has a unique solution which can be solved by iteration methods, e.g. the Newton–Raphson method. The algorithm for the Riemann problem to (1.1) and (2.3) is similar to the ones in [10, 11].

**4. Conclusions.** In this work we have constructed, in a unified framework, the complete exact solution of the Riemann problem for a $3 \times 3$ first-order system put forward as a simplified model for blood flow in medium to large arteries, with discontinuous material properties. The focus of the present work is on the subcritical Riemann initial data and backflows of collapsible tubes. On one hand, for the Riemann solution without collapsible vessel states, several examples are given for positive intermediate velocity. On the other hand, for solutions with collapsible vessel states, the examples are presented only for cases emerging due to the motion of the flow. The remaining possible solutions with the left or right initial collapsible tube states can be treated in the same manner.

REFERENCES


[1] J. Alastruey, W. Khir, K.S. Matthys, P. Segers, S.J. SherwinK, P.R. Verdonck, K.H. Parker, and J. Peiró",*Pulse wave propagation in a model human arterial network: Assessment of 1-D visco-elastic simulations against in vitro measurements.* J. Biomech., 44(2011), pp. 2250-2258.

[2] N. Andrianov and G. Warnecke,*On the solution to Riemann problem for compressible duct flow,* SIAM J. Appl. Math., 64(2004), pp. 878-901.

[3] N. Andrianov and G. Warnecke,*The Riemann problem for Baer-Nunziato model of two phase flows,* J. Comput. Phys., 195(2004) pp. 434-464.

[4] B. S. Brook, S. A. E. G: Falle, and T. J. Pedley, *Numerical solutions for unsteady gravity–driven flows in collapsible tubes: evolution and roll–wave instability of steady state*, J. Fluid Mech., 396(1999), pp. 223-256.

[5] S. Čanić, C.J. Hartley, D. Rosenstrauch, J. Tambača, G. Guidoboni, and A. Mikelić, *Blood flow in compliant arteries: an effective viscoelastic reduced model, numerical, and experimental validation*, Ann. Biomed. Eng., 34(2006), pp. 575-592.

[6] W. Dahmen, S. Müller, and A. Voss, *Riemann problem for the Euler equations with nonconvex equation of state including phase transitions,* Analysis and Numerics for Conservation Laws, Springer, Berlin, (2005), pp. 137-162.

[7] G. Dalmaso, P.L. LeFloch and F. Murat, *Definition and weak stability of non-conservative products*, J. Math. Pures. Appl., 74(1995), pp. 483-548.

[8] D. Elad, R.D. Kamm, and A.H. Shapiro, *Mathematical simulation of forced expiration*, J. Appl. Physiol., 65(1988), pp. 14-25.

[9] L. Formaggia, A. Quarteroni and A. Veneziani, Cardiovascular Mathematics, Modelling, simulation and application series. Springer-Verlag, Berlin, Heidelberg, New York, 2009.

[10] E. Han and G. Warnecke, *Exact Riemann solutions to shallow water equations*, Q. Appl. MATH. , accept, 2012.

[11] E. Han and M. Hantke and G. Warnecke, *Exact Riemann solutions in ducts with discontinuous cross-section*, J. Hyp. Diff. Equations, 9(2012), 403-449.

[12] E. Han, G. Warnecke, E. F. Toro and A Siviglia, *On Riemann solutions to weakly hyperbolic systems: Part 2. Modelling supercritical flows in arteries*, to be appeared .

[13] J. M. Hong, *An extension of Glimms method to inhomogeneous strictly hyperbolic systems of conservation laws by weaker than weak solutions of the Riemann problem*, J. Differential

Equations, 222(2006), pp. 515-549.
[14] J. Hong and B. Temple, *The Generic Solution of the Riemann Problem in a Neighborhood of a Point of Resonance for Systems of Nonlinear Balance Laws,* Methods Appl. Anal., 10(2003), pp. 279-294.
[15] E. Isaacson and B. Temple, *Nonlinear resonance in systems of conservation-laws*, SIAM J Appl. Math. 52(1992), pp. 1260-1278.
[16] R.D. Kamm and A.H. Shapiro , *Unsteady flow in a collapsible tube subjected to external pressure or body forces,* J. Fluid Mech., 95(1979), pp. 1-78.
[17] D.N. Ku,*Blood flow in arteries,* Annu. Rev. Fluid Mech., 129(1997), pp. 399-434.
[18] D.N. Ku, M.N. Zeigler, and J.M. Downing , *One-dimensional steady inviscid flow through a stenotic collapsible tube,* J. Biomech. Eng-T. ASME, 112(1990), pp. 444-450.
[19] P. G. Lefloch and M. D. Thanh, *The Riemann problem for fluid flows in a nozzle with discontinuous cross–section,* Commun. Maths. Sci., 1(2003), 763-797.
[20] P. G. LeFloch and M. D. Thanh, *The Riemann problem for shallow water equations with discontinuous Topography,* Commun. Maths. Sci., 5(2007), pp. 865-885.
[21] P. G. LeFloch and M. D. Thanh, *A Godunov-type method for the shallow water equations with discontinuous topography in the resonant regime,* J. Comput. Physics, 230(2011), pp. 7631-7660.
[22] R.J. LeVeque, Finite Volume Methods for Hyperbolic Problems, Cambridge University Press, 2002.
[23] F.Y. Liang, S. Takagi, R. Himeno, and H. Liu, *Biomechanical characterization of ventricular-arterial coupling during aging: a multi-scale model study,* J. Biomech., 42(2009) pp. 692-704.
[24] T. P. Liu, *Transonic gas flow in a duct of varying area.* Arch. Rat. Mech. Anal., 23(1982) pp. 1-18.
[25] T. P. Liu, *Nonlinear resonance for quasilinear hyperbolic equation,* J. Math. Phys., 28(1987) pp. 2593-2602.
[26] D. Marchesin and P. J. Paes-Leme, *A Riemann problem in gas dynamics with bifurcation,* Comp. Maths. Appls., 12(1986), pp. 433-455.
[27] T J. Pedley, The fluid dynamics of large blood vessels, Cambridge University Press, 1980.
[28] A. Quarteroni, M. Tuveri and A. Veneziani, *Computational vascular fluid dynamics: problems, models and methods,* Comp. Visual. Science, 2(2000), pp.63-197.
[29] A. Siviglia and M. Toffolon, *Steady analysis of transcritical flows in collapsible tubes with discontinuous mechanical properties: implications for arteries and veins,* J Fluid Mech., 7362013, pp. 195-215.
[30] M.D. Thanh, *The Riemann problem for a non-isentropic fluid in a nozzle with discontinuous cross-sectional area*, SIAM J. Appl. Math. , 69 (2009), pp. 1501-1519.
[31] E. F. Toro, Riemann solvers and numerical methods for fluid dynamics(3rd edition), Springer-Verlag, 2009
[32] E. F. Toro and A Siviglia, *Simplified blood flow model with discontinuous vessel properties: analysis and exact solutions. Modelling Physiological Flows Series: Modelling, Simulation and Applications. Editors: D. Ambrosi, A. Quarteroni and G. Rozza. Springer-Verlag,* 2011
[33] E. F. Toro and A Siviglia, *Flow in collapsible tubes with discontinuous mechanical properties: mathematical model and exact solutions. Commun. Comput. Phys.,* 13(2013), pp. 361-385.